

# Anchor Space Optimal Transport: Accelerating Batch Processing of Multiple OT Problems

Jianming Huang<sup>\*</sup>    Xun Su<sup>†</sup>    Zhongxi Fang<sup>‡</sup>    Hiroyuki Kasai<sup>§</sup>

October 26, 2023

## Abstract

The optimal transport (OT) theory provides an effective way to compare probability distributions on a defined metric space, but it suffers from cubic computational complexity. Although the Sinkhorn’s algorithm greatly reduces the computational complexity of OT solutions, the solutions of multiple OT problems are still time-consuming and memory-consuming in practice. However, many works on the computational acceleration of OT are usually based on the premise of a single OT problem, ignoring the potential common characteristics of the distributions in a mini-batch. Therefore, we propose a translated OT problem designated as the anchor space optimal transport (ASOT) problem, which is specially designed for batch processing of multiple OT problem solutions. For the proposed ASOT problem, the distributions will be mapped into a shared anchor point space, which learns the potential common characteristics and thus help accelerate OT batch processing. Based on the proposed ASOT, the Wasserstein distance error to the original OT problem is proven to be bounded by ground cost errors. Building upon this, we propose three methods to learn an anchor space minimizing the distance error, each of which has its application background. Numerical experiments on real-world datasets show that our proposed methods can greatly reduce computational time while maintaining reasonable approximation performance.

## 1 Introduction

As an important tool for comparing probability distributions, the optimal transport (OT) theory [1, 2] provides a robust and relevant distance for measuring two probability distributions on an already defined metric space, which is so-called the Wasserstein distance. However, due to the high computational complexity of  $O(n^3 \log(n))$  when solving the OT problem, it is difficult to apply it to practical machine learning tasks. In recent years, thanks to the computational improvements in solving OT problems with entropic regularizers, computing an approximate Wasserstein distance with a negligible error is brought down to a quadratic time complexity. Therefore, a lot of research works with applications of the OT theory showed up in many domains of machine learning, such as [3, 4], which introduced a mini-batch OT loss to the generative models. In the graph learning

---

<sup>\*</sup>Graduate School of Fundamental Science and Engineering, WASEDA University, 3-4-1 Okubo, Shinjuku-ku, Tokyo 169-8555, Japan (e-mail: koukenmei@toki.waseda.jp)

<sup>†</sup>Graduate School of Fundamental Science and Engineering, WASEDA University, 3-4-1 Okubo, Shinjuku-ku, Tokyo 169-8555, Japan (e-mail: suxun\_opt@asagi.waseda.jp)

<sup>‡</sup>Graduate School of Fundamental Science and Engineering, WASEDA University, 3-4-1 Okubo, Shinjuku-ku, Tokyo 169-8555, Japan (e-mail: fzx@akane.waseda.jp)

<sup>§</sup>Department of Computer Science and Communication Engineering, WASEDA University, 3-4-1 Okubo, Shinjuku-ku, Tokyo 169-8555, Japan (e-mail: hiroyuki.kasai@waseda.jp)

domain, a framework of the Wasserstein kernel was proposed, which utilizes the Wasserstein distance to define distances or embeddings between graph-structured data [5, 6]. In the sequence learning domain, [7] modified the original OT problem to generate a solution with the characteristic of sequential data by adding temporal regularization terms, while [8] proposed a method for sequence matching with three auto-weighted OT subproblems. In the meantime, in order to compute the solution to the OT problem more efficiently, many efforts have also been made. This includes related works such as the sliced Wasserstein distance [9, 10], which approximates the solution by solving one-dimensional OT problems on projections of data.

There exist many machine learning tasks that need to solve multiple OT problems as described in **Definition 1** of Section 2. For example, in a graph classification based on the Wasserstein graph kernels [5, 11, 12], we should compute a pairwise Wasserstein graph distance matrix in order to instantiate a precomputed kernel for the support vector machine. The pairwise Wasserstein graph distance matrix contains distances of every pair of graphs of the dataset, each of which is computed by solving a single OT problem. There are other similar examples such as the  $k$ -NN sequence classification task based on the order-preserving Wasserstein distance [7], and the distribution clustering tasks based on the Wasserstein distance [13, 14]. However, many works on the computational acceleration of OT are usually based on the premise of a single OT problem, without considering the batch processing acceleration of multiple OT problems. In this case, the conventional one-by-one computation, as shown at the left part of Figure 1, to compute a pairwise Wasserstein distance matrix is very inefficient because of the operation to instantiate the cost matrix ( $\mathbf{C}$  in Eq. (1)) for each distribution pair.

Although the Sinkhorn’s solver [2] provides a GPU-parallelizable solution to accelerate the OT batch processing, such operation is only applicable to distributions with fixed sizes. Under a situation where distributions are of different sizes, the OT batch processing becomes more difficult. Fortunately, this difficulty could be resolved by an improved Sinkhorn’s solver with a block-diagonal stacking strategy as described in Section 2.4. Nevertheless, it still requires more extra operations for block-diagonal stacking operations, and most importantly, it still cannot avoid the huge time and space cost caused by the cost matrix instantiation.

With considering the difficulties mentioned above, we assume that there exists some potential common characteristics among the distributions of the given dataset. With this assumption, we believe that conducting full-distribution transportations is unnecessary in batch processing, which will make the solution time-consuming and memory-consuming. Therefore, to resolve these difficulties, we propose a translated OT problem, where the distributions are transported based on an already learned and shared anchor point space. Thereafter, the original OT problem is converted to a lightweight one between a unique set of anchor points over the mapped distributions. As shown at the right part of Figure 1, because all the translated OT problems can share the same anchor point set, we do not need to instantiate the cost/kernel matrices for each of them, which helps to reduce much computational time and required memory for batch-processing. Moreover, because the distributions of the translated OT problems have a fixed size whether they are originally size-variable or not, it can be directly applicable to the Sinkhorn solver with GPU parallelization, without the need of the block-diagonal stacking. We name it the anchor space optimal transport (ASOT) problem. Furthermore, we derived and proved the upper bound of the Wasserstein distance error of our proposed ASOT problem to the original OT problem. We also proposed a metric learning framework (ASOT-ML) to learn the anchor space that minimizes the upper bound of Wasserstein distance error. However, we found that ASOT-ML has several limitations, which make it difficult to use under some conditions. Therefore, we further propose a lightweight version based on the  $k$ -means clustering (ASOT- $k$ ), and a deep dictionary learning version (ASOT-DL).

While there are similar works mapping distributions into anchor spaces or subspaces [15, 16],

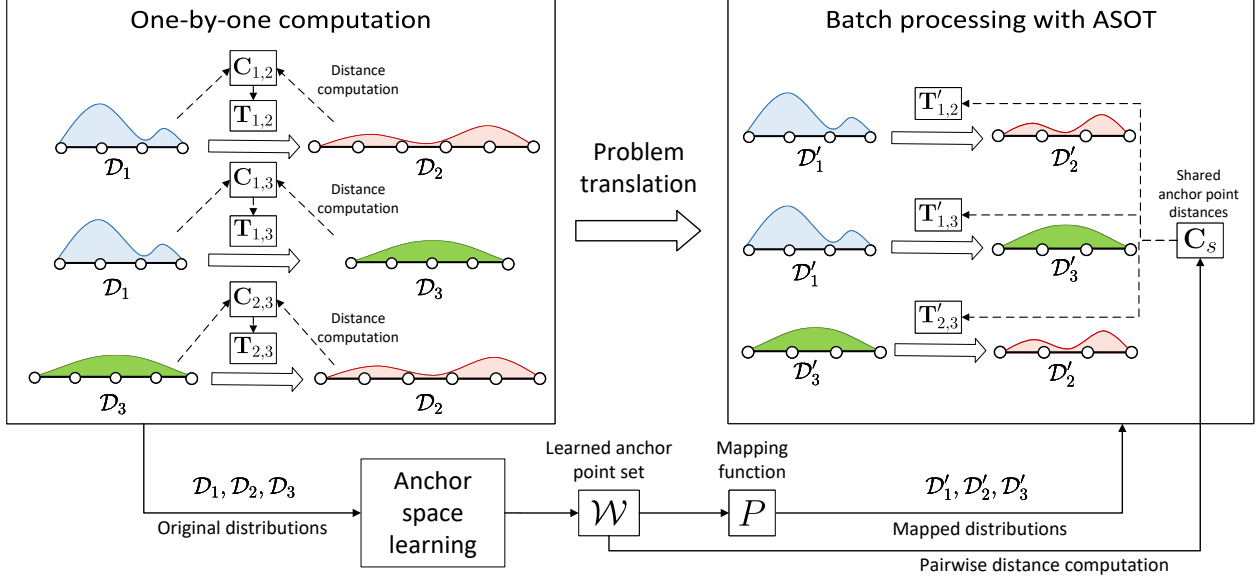


Figure 1: Illustration of the two strategies to solve multiple OT problems: the one-by-one computation (left) and the batch processing with the proposed ASOT problem (right). Assume a multiple OT problem set  $\mathcal{M}(\{\mathcal{D}_1, \mathcal{D}_2, \mathcal{D}_3\}, \{(1, 2), (1, 3), (2, 3)\})$ , let  $\mathbf{T}_{i,j}$  denotes the transportation plan from  $\mathcal{D}_i$  to  $\mathcal{D}_j$ . To solves the multiple problems, the conventional one-by-one computation needs the instantiation of cost matrices ( $\mathbf{C}_{1,2}, \mathbf{C}_{1,3}, \mathbf{C}_{2,3}$ ) for each distribution pairs. On the other hand, our proposed method learns an anchor space for all the distributions. Thereafter, the original distributions are mapped into the learned anchor space as  $\mathcal{D}'_1, \mathcal{D}'_2, \mathcal{D}'_3$ , which is a probability simplex based on a learnable anchor point set  $\mathcal{W}$ . When conducting batch processing with ASOT, all the translated OT problems share the same cost matrix  $\mathbf{C}_s$ , which is a pairwise distance matrix of the anchor points in  $\mathcal{W}$ . Therefore, there is no need to instantiate cost matrices for each distribution pairs.

these focus on enhancing OT’s robustness rather than considering multiple OT problems. For example, the latent OT [15] divides the OT problem into three subproblems of OT: source space to source anchor space, source anchor space to target anchor space, and target anchor space to target space, which costs much greater computational time than OT. Conversely, our proposed ASOT problem only contains one OT problem between the learned anchor points.

Our contributions are threefold: (i) We propose an anchor space optimal transport (ASOT) problem, which is translated from an optimal transport (OT) problem but benefits from no need of pairwise cost/kernel instantiation and the always fixed distribution size. The proposed ASOT greatly reduces the computational costs of the batch processing of multiple OT problems. (ii) We theoretically derived and proved the upper bound of the Wasserstein distance error between our ASOT and OT, which makes our approximation errors predictable. Moreover, to minimize such an upper bound, we propose three methods for anchor space learning (ASOT-ML, ASOT- $k$ , and ASOT-DL) for dealing with different situations. (iii) We evaluate distance approximation errors and computational time by conducting numerical experiments on several widely-used real-world datasets. These results show that our proposed approaches have a great reduction of computational time with reasonable approximation performances.

## 2 Preliminaries

We use lowercase letters to represent scalars, such as  $a, b$ , and  $c$ . Lowercase letters with bold typeface such as  $\mathbf{a}, \mathbf{b}, \mathbf{c}$  represent the vectors, uppercase letters with bold typeface such as  $\mathbf{A}, \mathbf{B}, \mathbf{C}$  represent the matrices. For the needs of slicing matrices, we represent the element of the  $i$ -th row and  $j$ -th columns of  $\mathbf{A}$  as  $\mathbf{A}(i, j)$ . Furthermore,  $\mathbf{A}(i, :)$  denotes the vector of  $i$ -th row of  $\mathbf{A}$ , similarly,  $\mathbf{A}(:, j)$  denotes the vector of  $j$ -th column.  $\mathbf{a}(i)$  denotes the  $i$ -th element of the vector  $\mathbf{a}$ . Uppercase letters with calligraphy typeface denote the set, such as  $\mathcal{A}, \mathcal{B}, \mathcal{C}$ ,  $|\mathcal{A}|$  denotes the size of  $\mathcal{A}$ .  $\mathbb{R}$  denotes the real number set,  $\mathbb{R}_+$  denotes the non-negative real number set.  $\mathbf{1}_n$  denotes an all-one vector.  $\langle \mathbf{A}, \mathbf{B} \rangle = \sum_{i,j} \mathbf{A}(i, j)\mathbf{B}(i, j)$  denotes the Frobenius dot product.  $\Delta_n^p := \{\mathbf{a} \in \mathbb{R}^n : a_i \geq 0, \sum_{i=1}^n a_i = 1\}$  denotes the  $n$ -dimensional probability simplex,  $\Delta_n^u := \{\mathbf{a} \in \mathbb{R}^n : a_i \geq 0, \sum_{i=1}^n a_i \leq 1\}$  denotes the  $n$ -dimensional unit simplex.  $[N]$  denotes the integer set  $\{1, 2, \dots, N\}$ .

### 2.1 Optimal transport (OT) problem

The optimal transport (OT) problem [1, 2] aims to find an OT plan between two probability measures defined on a given metric space. For the main topic discussed in this paper, we only consider the OT problem based on discrete probability distributions, which could be viewed as finite sets of sampling points with feature vectors. Assume that two discrete probability distributions on different simplexes are given as  $\mathbf{a} \in \Delta_n^p$  and  $\mathbf{b} \in \Delta_m^p$ . Assume that the sampling points of  $\mathbf{a}, \mathbf{b}$  are on the same metric space, where the distance between the sampling points could be measured by a given distance metric. Let  $\mathbf{C} \in \mathbb{R}^{n \times m}$  be the ground cost matrix where  $\mathbf{C}_{i,j}$  denotes the distance measured between the  $i$ -th sampling point of  $\mathbf{a}$  and  $j$ -th one of  $\mathbf{b}$ . The OT problem between  $\mathbf{a}$  and  $\mathbf{b}$  is defined as

$$\underset{\mathbf{T} \in \mathcal{U}(\mathbf{a}, \mathbf{b})}{\text{minimize}} \langle \mathbf{T}, \mathbf{C} \rangle, \quad (1)$$

where  $\mathcal{U}(\mathbf{a}, \mathbf{b}) = \{\mathbf{T} \in \mathbb{R}_+^{n \times m} : \mathbf{T}\mathbf{1}_m = \mathbf{a}, \mathbf{T}^T\mathbf{1}_n = \mathbf{b}\}$  denotes the set of all transportation plans between  $\mathbf{a}$  and  $\mathbf{b}$ . The OT problem derives a new distance measuring the optimal transportation cost named Wasserstein distance. The  $p$ -Wasserstein distance between two discrete probability distributions  $\mathbf{a}, \mathbf{b}$  is defined as  $W_p(\mathbf{a}, \mathbf{b}, \mathbf{C}) := \underset{\mathbf{T} \in \mathcal{U}(\mathbf{a}, \mathbf{b})}{\text{minimize}} \langle \mathbf{T}, \mathbf{C}^p \rangle^{\frac{1}{p}}$ . A wide application of the Wasserstein distance in specific machine learning tasks is to measure the 1-Wasserstein distance between two feature (sample) sets. Given two sets of  $d$ -dimensional features vectors  $\mathcal{X} = \{\mathbf{x}_i\}_{i=1}^n, \mathcal{Y} = \{\mathbf{y}_j\}_{j=1}^m$ , where  $\mathbf{x}_i, \mathbf{y}_j \in \mathbb{R}^d$ ,  $|\mathcal{X}| = n, |\mathcal{Y}| = m$  and their probability (mass) vector  $\mathbf{a} \in \Delta_n^p$  and  $\mathbf{b} \in \Delta_m^p$ , respectively. Let  $\mathcal{D}_x = (\mathcal{X}, \mathbf{a}), \mathcal{D}_y = (\mathcal{Y}, \mathbf{b})$  denotes the two distributions based on these two sample sets. To measure the optimal transportation cost between  $\mathcal{D}_x$  and  $\mathcal{D}_y$ , then the 1-Wasserstein distance between  $\mathcal{D}_x$  and  $\mathcal{D}_y$  is denoted as

$$W_1(\mathcal{D}_x, \mathcal{D}_y, d_S) := \underset{\mathbf{T} \in \mathcal{U}(\mathbf{a}, \mathbf{b})}{\text{minimize}} \langle \mathbf{T}, \mathbf{C} \rangle, \quad (2)$$

where  $d_S : \mathbb{R}^d \times \mathbb{R}^d \rightarrow \mathbb{R}_+$  denotes the given ground cost metric,  $\mathbf{C}(i, j) := d_S(\mathbf{x}_i, \mathbf{y}_j)$ . It should be noted that, because in a practical situation, there is usually no prior information about the probability distributions that are already known, there is a common way to set the probability vectors as uniform distributions as  $\mathbf{a} = \frac{\mathbf{1}_n}{n}, \mathbf{b} = \frac{\mathbf{1}_m}{m}$ .

### 2.2 Sinkhorn's algorithm

Because the OT problem expressed in Eq. (1) could be represented in the canonical form of a linear programming problem, which is a convex optimization problem, it can be solved in the complexity

of  $O(n^3 \log(n))$  in the case of  $n = m$ . Another more popular scheme for solving OT problems is Sinkhorn’s algorithm. Adding an entropic regularization term  $H(\mathbf{T}) := -\sum_{i,j} \mathbf{T}(i,j)(\log(\mathbf{T}(i,j)) - 1)$  to Eq. (1) obtains an entropically regularized OT (eOT) problem as

$$W_1^e(\mathcal{D}_x, \mathcal{D}_y) := \underset{\mathbf{T} \in \mathcal{U}(\mathbf{a}, \mathbf{b})}{\text{minimize}} \langle \mathbf{T}, \mathbf{C} \rangle - \varepsilon H(\mathbf{T}),$$

where  $\varepsilon > 0$  is a regularization paramter. This can be solved by introducing Sinkhorn’s fixed-point iterations in complexity of  $O(n^2 \log(n) \tau^{-3})$  with setting  $\varepsilon = \frac{4 \log(n)}{\tau}$  [17, 18, 19, 20]. In Sinkhorn’s algorithm, the transportation plan could be decomposed as  $\mathbf{T} = \mathbf{u}^T \mathbf{K} \mathbf{v}$ , where  $\mathbf{K} := \exp(-\frac{\mathbf{C}}{\varepsilon}) \in \mathbb{R}^{n \times m}$  is a Gibbs kernel computed from  $\mathbf{C}$  and  $\mathbf{u} \in \mathbb{R}_+^n, \mathbf{v} \in \mathbb{R}_+^m$  are two scaling variables to be updated. Then the updating equations of the  $j$ -th iteration of the Sinkhorn’s algorithm are defined as  $\mathbf{u}^{(j+1)} = \frac{\mathbf{a}}{\mathbf{K} \mathbf{v}^{(j)}}$  and  $\mathbf{v}^{(j+1)} = \frac{\mathbf{b}}{\mathbf{K}^T \mathbf{u}^{(j+1)}}$ .

### 2.3 Multiple optimal transport problem set

We present our definition of the multiple OT problem set, which is the main application scenario of the proposal.

**Definition 1** (Multiple optimal transport problem set). *Assume a discrete distribution set of size  $N$  as  $\mathbb{D} := \{\mathcal{D}_1, \dots, \mathcal{D}_N\}$ . Given a pair set  $\mathcal{P} \subset \{(i, j) : i, j \in [N], i \neq j\}$ , the multiple OT problem set is defined as*

$$\mathcal{M}(\mathbb{D}, \mathcal{P}) := \{W_1(\mathcal{D}_i, \mathcal{D}_j, d_S) : (i, j) \in \mathcal{P}; \mathcal{D}_i, \mathcal{D}_j \in \mathbb{D}\}, \quad (3)$$

where  $d_S : \mathbb{R}^d \times \mathbb{R}^d \rightarrow \mathbb{R}_+$  denotes the ground cost metric function.  $d$  denotes the number of dimensions of each sample.

Problems of the multiple OT problem set can be viewed as single OT problems of the given distribution set  $\mathbb{D}$ . For the cases where distributions in  $\mathbb{D}$  are of the same size, such problems can be solved parallelly with the GPU-parallelizable Sinkhorn’s algorithm. When distribution sizes are allowed to vary, we cannot directly utilize the GPU-parallelizable Sinkhorn’s algorithm and should instead utilize the block-diagonal stacking strategy.

### 2.4 The block-diagonal stacking strategy

Under the condition of size-fixed distributions, the updating equations of the Sinkhorn’s algorithm can be easily batched with stacking  $\mathbf{u}, \mathbf{v}, \mathbf{a}, \mathbf{b}$  and  $\mathbf{K}$  along a new batch dimension to create a volume. Although this strategy is inapplicable to size-variable distributions, we can adopt a block-diagonal stacking strategy where the kernel matrices  $\mathbf{K}$  are stacked along the diagonal, while other vectors are stacked vertically instead of creating a new dimension. Thereafter, substituting the batched matrices and vectors into the original equation obtains a matrix of batched solutions. Such batch processing is also efficiently GPU-parallelizable with the release of dedicated CUDA kernels [21].

## 3 Anchor Space Optimal Transport (ASOT)

This section introduces the definition of our proposed ASOT problem. We then present the theorem of upper bound of absolute 1-Wasserstein distance error between ASOT and normal OT.

### 3.1 Motivation and definitions

As described in the previous sections, there are two weak points of the conventional one-by-one computation that we focus on: (i) the need of cost matrices instantiation for every distribution pairs; (ii) the need of extra operations to parallelize with size-variable distributions. To resolve these two difficulties, we believe that we can take advantages of some potential common characteristics of the given distributions in the multiple OT problem set. In order to remove the cost matrices instantiation described in (i), we design a so-called ASOT problem to approximate the original OT problem. It can be viewed as a new one with a low-rank representation of the original cost matrix. The most important point is that it has a fixed and shareable component (**Lemma 1**). For the difficulty of (ii), in our proposed ASOT problem, the transportation is only based on the distributions of the learned anchor point set, which have the fixed size equal to the number of anchor points, thus do not require the operation of block-diagonal stacking. In summary, we propose to learn a so-called anchor space for a batch of distributions that allow variable size, over which our defined ASOT problems could be solved efficiently. Meanwhile, it also has an upper bounded cost error to the original OT problem. We present the relative definitions of ASOT as follows:

**Definition 2** (Anchor space). *Assume a metric space on  $\mathbb{R}^d$  with a metric function  $d_{AS} : \mathbb{R}^d \times \mathbb{R}^d \rightarrow \mathbb{R}_+$ , denoted as  $S(\mathbb{R}^d, d_{AS})$ . Let  $\mathcal{W} = \{\mathbf{w}_i\}_{i=1}^k$  be a set of  $k$  points on  $S(\mathbb{R}^d, d_{AS})$ , where  $\mathbf{w}_i \in \mathbb{R}^d$ . An anchor space of  $\mathcal{W}$  is defined as a  $k$ -dimensional probability simplex, denoted as  $S_A(\mathcal{W}) = \Delta_k^p$ . The points of  $\mathcal{W}$  are called the anchor points.*

**Definition 3** (Anchor space optimal transport (ASOT) problem). *Let  $d_S, d_{AS} : \mathbb{R}^d \times \mathbb{R}^d \rightarrow \mathbb{R}_+$  be two metric functions on  $\mathbb{R}^d$ . Assume two discrete distributions  $\mathcal{D}_x = (\mathcal{X}, \mathbf{a}), \mathcal{D}_y = (\mathcal{Y}, \mathbf{b})$  on a source metric space  $S(\mathbb{R}^d, d_S)$ , where  $\mathcal{X} = \{\mathbf{x}_i\}_{i=1}^n, \mathcal{Y} = \{\mathbf{y}_j\}_{j=1}^m$  denotes the sample sets and  $\mathbf{x}_i, \mathbf{y}_j \in \mathbb{R}^d$ ,  $\mathbf{a} \in \Delta_n^p, \mathbf{b} \in \Delta_m^p$  denotes their probability (mass) vectors, respectively. Given a set of  $k$  anchor points  $\mathcal{W} = \{\mathbf{w}_i\}_{i=1}^k$  on a new metric space  $S(\mathbb{R}^d, d_{AS})$ , where  $\mathbf{w}_i \in \mathbb{R}^d$ . And given a mapping function  $P : \mathbb{R}^d \rightarrow S_A(\mathcal{W})$ . Then, we define the 1-Wasserstein distance of ASOT problem over the anchor space  $S_A(\mathcal{W})$  as*

$$W_{AS}(\mathcal{D}_x, \mathcal{D}_y, \mathcal{W}, P, d_{AS}) := \underset{\mathbf{T}_s \in \mathcal{U}(\mathbf{a}', \mathbf{b}')}{\text{minimize}} \langle \mathbf{T}_s, \mathbf{C}_s \rangle, \quad (4)$$

$$\mathbf{a}' = \frac{1}{n} \sum_{i=1}^n P(\mathbf{x}_i) \mathbf{a}(i), \quad \mathbf{b}' = \frac{1}{m} \sum_{j=1}^m P(\mathbf{y}_j) \mathbf{b}(j), \quad (5)$$

where  $W_{AS}(\mathcal{D}_x, \mathcal{D}_y, \mathcal{W}, P, d_{AS})$  denotes the 1-Wasserstein distance of the ASOT problem, and  $\mathbf{T}_s \in \mathbb{R}^{k \times k}$  denotes the transportation plan between the anchor points of  $\mathcal{W}$ .  $\mathbf{C}_s \in \mathbb{R}^{k \times k}$  denotes the pairwise cost matrix of the anchor points of  $\mathcal{W}$ , where  $\mathbf{C}_s(i, j) := d_{AS}(\mathbf{w}_i, \mathbf{w}_j)$ .

We further define an entropic variant of the ASOT problem envisioning the application of Sinkhorn's algorithm for GPU parallelization.

**Definition 4** (Entropic anchor space optimal transport (eASOT) problem). *Follow the same definitions of **Definition 3**. Then, an entropic variant problem of Eq. (4) is defined as*

$$W_{AS}^e(\mathcal{D}_x, \mathcal{D}_y, \mathcal{W}, P, d_{AS}) := \underset{\mathbf{T}_s \in \mathcal{U}(\mathbf{a}, \mathbf{b})}{\text{minimize}} \langle \mathbf{T}_s, \mathbf{C}_s \rangle - \varepsilon H(\mathbf{T}_s). \quad (6)$$

*This is called the entropic ASOT problem denoted as eASOT.*

### 3.2 Properties of ASOT

In this subsection, we show several important and useful properties of our proposed ASOT.

**ASOT meets the definition of an OT problem.** Reviewing the definition of an OT problem, it is obvious that ASOT is also an OT problem over two new distributions  $\mathcal{D}'_x = (\mathcal{W}, \mathbf{a}')$ ,  $\mathcal{D}'_y = (\mathcal{W}, \mathbf{b}')$  with a ground cost matrix  $\mathbf{C}_s$  computed by a distance measure  $d_{AS}$ . This property allows us to solve an ASOT problem in the same way as OT does. The minimum cost of the ASOT problem is also guaranteed to have the same properties as the 1-Wasserstein distance.

**ASOT always has fixed distribution sizes.** As shown in the equations of **Definition 3**, the sizes of distributions  $\mathcal{D}'_x, \mathcal{D}'_y$ , the transportation plan  $\mathbf{T}_s$  and the cost matrix  $\mathbf{C}_s$  are always fixed, which only depends on the anchor space  $S_A(\mathcal{W})$ . Therefore, this property makes the eASOT problem efficiently solvable with GPU parallelization.

**Upper bounded error to OT.** In order to translate an arbitrary OT problem into the form of our proposed ASOT problem with ensuring a controllable cost error. We present the upper bound of their absolute 1-Wasserstein distance error as the following **Proposition 1**. Before that, we first prepare the following **Lemma 1**, which also reveals another important property of our proposed ASOT problem: its equivalence to a specific OT problem of uniform distributions.

**Lemma 1** (Equivalence lemma). *The following OT problem is equivalent to the ASOT problem  $W_{AS}(\mathcal{D}_x, \mathcal{D}_y, \mathcal{W}, P, d_{AS})$ , where  $\hat{\mathbf{C}} = \mathbf{Z}_x \mathbf{C}_s \mathbf{Z}_y^T$ .*

$$\underset{\mathbf{T} \in \mathcal{U}(\mathbf{a}, \mathbf{b})}{\text{minimize}} \langle \mathbf{T}, \hat{\mathbf{C}} \rangle, \quad (7)$$

where  $\mathcal{D}_x = (\mathcal{X}, \mathbf{a})$ ,  $\mathcal{D}_y = (\mathcal{Y}, \mathbf{b})$ .

*Proof.* Let  $W_T := \langle \mathbf{T}, \hat{\mathbf{C}} \rangle$  in Eq. (7). It can be rewritten as following equation with substituting  $\hat{\mathbf{C}} = \mathbf{Z}_x \mathbf{C}_s \mathbf{Z}_y^T$  into it.

$$W_T = \sum_{u, v \in [k]} \sum_{i \in [n], j \in [m]} \mathbf{Z}_x(i, u) \cdot \mathbf{Z}_y(j, v) \cdot \mathbf{T}(i, j) \cdot \mathbf{C}_s(u, v).$$

Let  $\mathbf{T}_s = \mathbf{Z}_x^T \mathbf{T} \mathbf{Z}_y \in \mathbb{R}^{k \times k}$ , where  $k := |\mathcal{W}|$  denotes the number of anchor points. Substituting it into the above equation obtains

$$W_T = \sum_{u, v \in [k]} \sum_{i, j \in [k]} \mathbf{T}_s(i, j) \cdot \mathbf{C}_s(u, v) = \langle \mathbf{T}_s, \mathbf{C}_s \rangle.$$

Substituting it into Eq. (7) obtains  $\underset{\mathbf{T} \in \mathcal{U}(\mathbf{a}, \mathbf{b})}{\text{minimize}} \langle \mathbf{T}_s, \mathbf{C}_s \rangle$ . To reparameterize this problem with  $\mathbf{T}_s$ , we first right multiply it with  $\mathbf{1}_k$ . Then we have  $\mathbf{T}_s \mathbf{1}_k = \mathbf{Z}_x^T \mathbf{T} \mathbf{Z}_y \mathbf{1}_k$ . Furthermore, because each row of  $\mathbf{Z}_x$  and  $\mathbf{Z}_y$  is a simplex vector, we have  $\mathbf{Z}_y \mathbf{1}_k = \mathbf{1}_m$ . Then we have  $\mathbf{T}_s \mathbf{1}_k = \mathbf{Z}_x^T \mathbf{T} \mathbf{1}_m = \frac{1}{n} \mathbf{Z}_x^T \mathbf{a} = \mathbf{a}'$ , where  $\mathbf{a}'$  denotes the same one in **Definition 3**. In the same way, we can obtain  $\mathbf{T}_s^T \mathbf{1}_k = \mathbf{b}'$ , where  $\mathbf{b}'$  denotes the same one in **Definition 3**. Finally, Eq. (7) can be rewritten as follows.

$$\underset{\mathbf{T}_s \in \mathcal{U}(\mathbf{a}', \mathbf{b}')}{\text{minimize}} \langle \mathbf{T}_s, \mathbf{C}_s \rangle.$$

□

**Proposition 1** (Upper bound of the absolute 1-Wasserstein distance error). *Assume an OT problem for 1-Wasserstein distance  $W_1(\mathcal{D}_x, \mathcal{D}_y, d_S)$ , with  $\mathbf{C} \in \mathbb{R}^{n \times m}$  as the ground cost matrix and  $d_S$  as the metric function. Define an ASOT problem  $W_{AS}(\mathcal{D}_x, \mathcal{D}_y, \mathcal{W}, P, d_{AS})$  of **Definition 3** with given*

$\mathcal{W}, P$  and  $d_{AS}$ . Let  $\mathbf{Z}_x \in \mathbb{R}^{n \times k}, \mathbf{Z}_y \in \mathbb{R}^{m \times k}$  be the matrices where  $\mathbf{Z}_x(i, :) = P(\mathbf{x}_i), \mathbf{Z}_y(j, :) = P(\mathbf{y}_j)$ . We define a reconstructed cost matrix  $\widehat{\mathbf{C}} = \mathbf{Z}_x \mathbf{C}_s \mathbf{Z}_y^T \in \mathbb{R}^{n \times m}$ . Then the following inequality holds.

$$|W_{AS}(\mathcal{D}_x, \mathcal{D}_y, \mathcal{W}, P, d_{AS}) - W_1(\mathcal{D}_x, \mathcal{D}_y, d_S)| < \|\widehat{\mathbf{C}} - \mathbf{C}\|_1. \quad (8)$$

*Proof.* Let  $\mathbf{T}^*, \widehat{\mathbf{T}}^*$  be the optimal  $\mathbf{T}$  of Eqs. (2) and (7), respectively. According to **Lemma 1**, we have  $|W_{AS} - W_1| = |\sum_{i,j} \widehat{\mathbf{T}}^*(i, j) \widehat{\mathbf{C}}(i, j) - \sum_{i,j} \mathbf{T}^*(i, j) \mathbf{C}(i, j)|$ . In the case of  $W_{AS} > W_1^u$ , we have the following inequalities.

$$\begin{aligned} |W_{AS} - W_1| &= \sum_{i,j} \widehat{\mathbf{T}}^*(i, j) \widehat{\mathbf{C}}(i, j) - \sum_{i,j} \mathbf{T}^*(i, j) \mathbf{C}(i, j) \\ &\leq \sum_{i,j} \mathbf{T}^*(i, j) (\widehat{\mathbf{C}}(i, j) - \mathbf{C}(i, j)) \\ &\leq \sum_{i,j} \mathbf{T}^*(i, j) |\widehat{\mathbf{C}}(i, j) - \mathbf{C}(i, j)| \\ &< \|\widehat{\mathbf{C}} - \mathbf{C}\|_\infty < \|\widehat{\mathbf{C}} - \mathbf{C}\|_1. \end{aligned}$$

In the case of  $W_{AS} \leq W_1$ , we have  $|W_{AS} - W_1| = |\sum_{i,j} \mathbf{T}^*(i, j) \mathbf{C}(i, j) - \sum_{i,j} \widehat{\mathbf{T}}^*(i, j) \widehat{\mathbf{C}}(i, j)|$ . Replacing  $\mathbf{T}^*(i, j)$  in the 2nd and the 3rd rows above with  $\widehat{\mathbf{T}}^*(i, j)$  can obtain the desired result.  $\square$

The above two proofs are both proof sketches, while the complete proofs of **Lemma 1** and **Proposition 1** are included in the supplementary file. Based on **Proposition 1**, we can translate a given OT problem into an ASOT problem by minimizing the upper bound  $\|\widehat{\mathbf{C}} - \mathbf{C}\|_1$ , which can be viewed as a function of three variables  $\mathcal{W}, P$  and  $d_{AS}$ . To solve this optimization problem, we propose three methods for different application backgrounds, one of which is based on the metric learning and the other two are based on  $k$ -means clustering and the deep dictionary learning, which will be discussed in Section 4.

### 3.3 GPU-parallelizable Sinkhorn for eASOT problem

We have already introduced the definition of the ASOT problem on a single pair of distributions in the previous subsection. In the case of GPU parallelization on a multiple OT problem set, we consider computing their 1-Wasserstein distances by solving the translated eASOT problems over a shared anchor space of  $\mathcal{W}$  and metric function  $d_{AS}$ . In this case, all of the distribution pairs in the batch share a set of parameters of  $\mathcal{W}, P$  and  $d_{AS}$ , which only need to be learned once. According to **Remark 4.16** in [2], we use the GPU parallelization version of the Sinkhorn's algorithm to solve the eASOT problem. More concretely, given  $N$  translated probability distribution pairs of ASOT  $\{(\mathbf{a}_i, \mathbf{b}_i)\}_{i=1}^N$ , where  $\mathbf{a}_i, \mathbf{b}_i \in \mathbb{R}^k$ , and  $\mathbf{A} := [\mathbf{a}_1, \dots, \mathbf{a}_N] \in \mathbb{R}^{k \times N}, \mathbf{B} := [\mathbf{b}_1, \dots, \mathbf{b}_N] \in \mathbb{R}^{k \times N}$ , the following equation updates the dual variables  $\mathbf{u}_i \in \mathbb{R}^k$  and  $\mathbf{v}_i \in \mathbb{R}^k$  at the  $j$ -th iteration of Sinkhorn's algorithm with GPU parallelization.

$$\mathbf{U}^{(j+1)} = \frac{\mathbf{A}}{\mathbf{K}\mathbf{V}^{(j)}}, \quad \mathbf{V}^{(j+1)} = \frac{\mathbf{B}}{\mathbf{K}^T \mathbf{U}^{(j+1)}},$$

where  $\mathbf{U} := [\mathbf{u}_1, \dots, \mathbf{u}_N], \mathbf{V} := [\mathbf{v}_1, \dots, \mathbf{v}_N] \in \mathbb{R}^{k \times N}$ , and  $\mathbf{K} := \exp(-\frac{\mathbf{C}_s}{\epsilon}) \in \mathbb{R}^{k \times k}$  is the Gibbs kernel.



### 3.4 Complexity analysis

We present a comparison of the time and space complexity of the one-by-one computation and the batch processing of our ASOT problem with the Sinkhorn’s solver. Let  $N$  denote the number of distributions in the mini-batch, and let  $s$  denote the average number of samples in a distribution.

**Time complexity.** For the preparation procedure before Sinkhorn’s algorithm, the one-by-one computation requires an  $O(Ns^2)$  computation to instantiate kernels, while ASOT only requires  $O(Ns)$  to map distributions with mapping function  $P$ . For the Sinkhorn’s procedure, the one-by-one computation requires an  $O(s^3)$  to compute  $\mathbf{K}\mathbf{v}$  and  $\mathbf{K}^T\mathbf{u}$  for each single Sinkhorn loop. ASOT, on the other hand, requires  $O(k^3)$ , where  $k$  denotes the number of anchor points. It should be noted that the Sinkhorn’s algorithm with block diagonal stacking has an extra operation to extract the results from the block diagonal matrix with batch indices in the case of different distribution sizes. On the other hand, our proposed ASOT with the stacking methods described in Section 3.3 does not require such operation.

**Space complexity.** The one-by-one computation requires an  $O(Ns^2)$  space for restoring every cost matrix, while ASOT only requires  $O(k^2)$ . Therefore, with setting  $k$  and  $s$  at the same level of magnitude, the ASOT will save much space and make it able to create a mini-batch of a larger size, which can also accelerate computation under a limited memory size.

## 4 Anchor Space Learning

As mentioned above, to translate OT problems into ASOT problems, we need to learn an anchor space to minimize the upper bound in **Proposition 1** w.r.t.  $\mathcal{W}, P$  and  $d_{AS}$ . This section presents a deep metric learning framework, a  $k$ -means-based framework, and a deep dictionary learning framework to solve this optimization problem. Each has different advantages and disadvantages, which will be discussed in this section.

### 4.1 Deep metric learning ASOT (ASOT-ML)

For the framework of our metric learning ASOT, to minimize  $\|\widehat{\mathbf{C}} - \mathbf{C}\|_1$ , we first assume that  $\widehat{\mathbf{C}}$  is computed by a parameterized metric function  $f(\mathcal{W}, P, d_{AS})$ , defined as follows.

$$\begin{aligned} \widehat{\mathbf{C}}(i, j) &= f(\mathcal{W}, P, d_{AS}) \\ &= \sum_{u, v \in [k]} \mathbf{Z}_x(i, u) \cdot \mathbf{Z}_y(j, u) \cdot d_{AS}(\mathbf{w}_u, \mathbf{w}_v) \\ &= \sum_{u, v \in [k]} P(\mathbf{x}_i)(u) \cdot P(\mathbf{y}_j)(v) \cdot d_{AS}(\mathbf{w}_u, \mathbf{w}_v). \end{aligned}$$

Then the problem becomes a metric learning problem from  $f$  to  $d_S$ , which is the ground metric function of  $\mathbf{C}$ . Because we have two variables  $P$  and  $d_{AS}$  that are functions, we parameterize  $P$  with a multilayer perceptron network (MLP); we use the Mahalanobis distance for  $d_{AS}$ , which is computed as  $d_{AS}(\mathbf{w}_u, \mathbf{w}_v) = \|\mathbf{M}\mathbf{w}_u - \mathbf{M}\mathbf{w}_v\|_2$ , where  $\mathbf{M} \in \mathbb{R}^{h \times k}$  is a learned parameter matrix,  $h$  denotes the number of the hidden dimensions. It should be noted that, in order to ensure that the outputs of  $P$  are within the probability simplex, the outputs of the MLP for  $P$  are normalized by dividing their  $l_1$  norms. Thereafter, we adopt an automatic differentiation neural network system to build our framework, as shown at (a) in Figure 2. The loss function for the framework is defined as  $l(i, j) = |f(\mathcal{W}, P, d_{AS}) - d_S(\mathbf{x}_i, \mathbf{y}_j)|$  for each pair of sampling points. To avoid the subgradient, we adopt an  $l_2$  loss as  $l_{ML} = \frac{C}{nm} \sum_{i \in [n], j \in [m]} l(i, j)^2$ , where  $C$  is a scalar.

However, there exist several limitations for ASOT-ML: (i) Quadratic complexity: Because ASOT-ML needs pairwise distance errors, it has both time complexity and space complexity of  $O(n^2)$ . Therefore, it is impossible to conduct full pairwise distance computation on a large-scale dataset but have to use mini-batch pairwise distances, which might affect its performance. (ii) Unsafe solution: ASOT-ML can not control the scale of the learned cost matrix, which might cause a risk of overflow while computing Sinkhorn’s algorithm. It is because when  $\mathbf{C}_s$  has a too large or too small value, the computation of  $\mathbf{K} = \exp(-\frac{\mathbf{C}_s}{\epsilon})$  will produce outliers and thus affects the updating process.

## 4.2 $k$ -means-based (ASOT- $k$ ) and Deep dictionary learning ASOT (ASOT-DL)

**Upper bound under the one-hot condition.** In order to avoid the limitations of ASOT-ML, we propose a relative lightweight deep dictionary learning framework based on several special conditions, which only has a complexity of  $O(n)$  level. We present the following proposition of upper bound and provide its proof sketch, while the complete proof is in the supplementary file.

**Proposition 2** (Upper bound of absolute 1-Wasserstein error under the one-hot condition). *Let  $\mathbf{q}_a^b \in \mathbb{R}^a$  denotes an  $a$ -dimensional one-hot vector of which the  $b$ -th element is equal to 1, i.e.  $\mathbf{q}_a^b(b) = 1$ . Let  $P_o : \mathbb{R}^d \rightarrow \{\mathbf{q}_k^i\}_{i=1}^k$  be an one-hot mapping function, let  $\mathcal{W} = \{\mathbf{w}_i\}_{i=1}^k$  and  $\mathbf{W} = [\mathbf{w}_1, \dots, \mathbf{w}_k] \in \mathbb{R}^{d \times k}$ . Given two discrete distributions  $\mathcal{D}_x = (\mathcal{X}, \mathbf{a}), \mathcal{D}_y = (\mathcal{Y}, \mathbf{b})$ , where  $\mathcal{X} = \{\mathbf{x}_i\}_{i=1}^n, \mathcal{Y} = \{\mathbf{y}_j\}_{j=1}^m, \mathbf{x}_i, \mathbf{y}_j \in \mathbb{R}^d$ , and  $\mathbf{a} \in \Delta_n^p, \mathbf{b} \in \Delta_m^p$ . Assume an original OT problem  $W_1(\mathcal{D}_x, \mathcal{D}_y, d_E)$ , which is translated into an ASOT problem as  $W_{AS}(\mathcal{D}_x, \mathcal{D}_y, \mathcal{W}, P_o, d_E)$ , where  $d_E$  is the Euclidean distance function. Then the following inequality holds.*

$$|W_{AS}(\mathcal{D}_x, \mathcal{D}_y, \mathcal{W}, P_o, d_E) - W_1(\mathcal{D}_x, \mathcal{D}_y, d_E)| < m \sum_{i \in [n]} \|\epsilon_i^x\|_2 + n \sum_{j \in [m]} \|\epsilon_j^y\|_2,$$

where  $\epsilon_i^x = \mathbf{W}P_o(\mathbf{x}_i) - \mathbf{x}_i, \epsilon_j^y = \mathbf{W}P_o(\mathbf{y}_j) - \mathbf{y}_j$  denote the offsets of reconstructed features to the original ones.

*Proof.* Let  $\eta := |W_{AS} - W_1|$ , where  $W_{AS} := W_{AS}(\mathcal{D}_x, \mathcal{D}_y, \mathcal{W}, P_o, d_E)$ , and  $W_1 := W_1(\mathcal{D}_x, \mathcal{D}_y, d_E)$ . From **Proposition 1**, we have

$$\begin{aligned} \eta &< \|\widehat{\mathbf{C}} - \mathbf{C}\|_1 \\ &< \sum_{i \in [n], j \in [m]} \left| \widehat{\mathbf{C}}(i, j) - \mathbf{C}(i, j) \right| \\ &< \sum_{i \in [n], j \in [m]} \left| \sum_{u, v \in [k]} \mathbf{z}_i^x(u) \cdot \mathbf{z}_j^y(v) \cdot \mathbf{C}_s(u, v) - \mathbf{C}(i, j) \right|, \end{aligned}$$

where  $\mathbf{z}_i^x := P_o(\mathbf{x}_i), \mathbf{z}_j^y := P_o(\mathbf{y}_j)$ . Because  $P_o$  is an one-hot mapping function, we can let the index of non-zero element of  $P_o(\mathbf{x}_i)$  be  $u_i$ , and let the one of  $P_o(\mathbf{y}_j)$  be  $v_j$ . Substituting this into the inequalities above obtains

$$\eta < \sum_{i \in [n], j \in [m]} |\mathbf{C}_s(u_i, v_j) - \mathbf{C}(i, j)|.$$

From **Definition 3**, we have  $\mathbf{C}_s(u_i, v_j) = d_E(\mathbf{w}_{u_i}, \mathbf{w}_{v_j}) = \|\mathbf{w}_{u_i} - \mathbf{w}_{v_j}\|_2$  and  $\mathbf{C}(i, j) = d_E(\mathbf{x}_i, \mathbf{y}_j) = \|\mathbf{x}_i - \mathbf{y}_j\|_2$ . Let  $\epsilon_i^x := \mathbf{W}P_o(\mathbf{x}_i) - \mathbf{x}_i, \epsilon_j^y := \mathbf{W}P_o(\mathbf{y}_j) - \mathbf{y}_j$ . Then,  $\epsilon_i^x = \mathbf{w}_{u_i} - \mathbf{x}_i, \epsilon_j^y = \mathbf{w}_{v_j} - \mathbf{y}_j$ . Substituting these into the inequality above obtains

$$\eta < \sum_{i \in [n], j \in [m]} \left| \|\mathbf{w}_{u_i} - \mathbf{w}_{v_j}\|_2 - \|(\mathbf{w}_{u_i} - \mathbf{w}_{v_j}) + (\epsilon_j^y - \epsilon_i^x)\|_2 \right|.$$

According to the reverse triangle inequality [22], we have

$$\begin{aligned}
\eta &< \sum_{i \in [n], j \in [m]} \|\epsilon_j^y - \epsilon_i^x\|_2 \\
&< \sum_{i \in [n], j \in [m]} \|\epsilon_j^y\|_2 + \|\epsilon_i^x\|_2 \\
&< m \sum_{i \in [n]} \|\epsilon_i^x\|_2 + n \sum_{j \in [m]} \|\epsilon_j^y\|_2,
\end{aligned}$$

□

From **Proposition 2**, with a special one-hot encoding  $P_o$  and a shared  $l_p$  norm distance function  $d_S$  for both anchor space and original space, the distance error could be upper bounded within a summation of reconstruction errors. In this case, there are only two parameters to be learned, which are  $\mathcal{W}$  and  $P_o$ . Both our proposed ASOT- $k$  and ASOT-DL methods are based on the same optimization problem derived from **Proposition 2**, which is  $\text{minimize}_{\mathcal{W}, P_o} \sum_{i \in [n]} \|\epsilon_i^x\|_2 + \sum_{j \in [m]} \|\epsilon_j^y\|_2$ . This optimization problem only needs computation of  $O(n + m)$  complexity. Furthermore, for the limitation of the unsafe solution, because of the one-hot constraint and the share of the metric function  $d_S$  over both the anchor space and the original space, the learned cost matrix of anchor points  $\mathbf{C}_s$  usually has the same scale as the one of original OT problem  $\mathbf{C}$ . Therefore, it is less likely to provide unsafe solutions with **Proposition 2**. The last, because **Proposition 2** is built upon extra conditions from **Proposition 1**, its solution set should be included in the later one. Therefore, theoretically, ASOT-ML can have better solutions than ASOT- $k$  and ASOT-DL.

By minimizing the reconstruction errors, the problem becomes a classical clustering problem or a dictionary learning problem. For a clustering problem, it could be easily solved with the  $k$ -means algorithm and its variants, where  $\mathcal{W}$  is the set of cluster centers and  $P_o$  is the clustering operator. Therefore, we utilize the  $k$ -means algorithm to learn the anchor space in our ASOT- $k$  method. However, the one-hot condition might be too strict, which makes it less possible to achieve low reconstruction errors. Therefore, We also propose a deep dictionary learning framework ASOT-DL to optimize a near-one-hot mapping function. In more detail, we adopt a framework from [23], named deep K-SVD, with adding some modifications to fit our conditions.

**Total loss for deep dictionary learning.** We first elaborate on the definition of the total loss for our deep dictionary learning framework before the details of the network structure. Let  $\mathbf{x}_i \in \mathbb{R}^d$  be a  $d$ -dimensional sampling point,  $\mathbf{X} := [\mathbf{x}_1, \mathbf{x}_2, \dots, \mathbf{x}_n]^T \in \mathbb{R}^{n \times d}$ . Let  $\mathbf{z}_i = P_o(\mathbf{x}_i) \in \mathbb{R}^k$  be a near-one-hot encoding for  $\mathbf{x}_i$ ,  $\mathbf{Z} := [\mathbf{z}_1, \dots, \mathbf{z}_n]^T \in \mathbb{R}^{n \times k}$ . Given an anchor point matrix  $\mathbf{W} = [\mathbf{w}_1, \dots, \mathbf{w}_k] \in \mathbb{R}^{d \times k}$ , we first define a total loss  $l$  for our deep dictionary learning framework as  $l(\mathbf{W}, \mathbf{Z}) := \alpha \cdot l_{rc} + \beta \cdot l_{lp} + \gamma \cdot l_{sp}$ , where  $l_{rc}$ ,  $l_{lp}$ , and  $l_{sp}$  are a reconstruction loss, an  $l_p$ -ball loss, and a simplex constraint violation loss, respectively.  $\alpha, \beta, \gamma \in \mathbb{R}_+$  denote the weights of their corresponding losses. These losses are computed as  $l_{rc} := \frac{1}{2n} \sum_{i=1}^n \|\mathbf{W}(\mathbf{Z}(i, :))^T - (\mathbf{X}(i, :))^T\|_2^2$ ,  $l_{lp} := \frac{1}{n} \sum_{i=1}^n (\|\mathbf{Z}(i, :)\|_p - 1)^2$ ,  $l_{sp} := \frac{1}{n} \sum_{i=1}^n (\mathbf{Z}(i, :)\mathbf{1}_k - 1)^2$ , where  $p > 1$  is a scalar. For the  $l_p$ -ball loss and the simplex constraint violation loss, they penalize the learned near-one-hot codings to constrain them within an intersection of the surface of a unit  $l_p$ -ball ( $p > 1$ ) and a unit simplex  $\Delta_k^u$ , which is the one-hot vector set  $\{\mathbf{q}_k^i\}_{i=1}^k$ .

**Details of the framework structure.** In the original paper of deep K-SVD, they proposed a deep dictionary learning model based on the ISTA algorithm [24] with an adapted  $\lambda$ , which is actually a sparse encoder. The ISTA algorithm solves the lasso problem  $\text{minimize}_{\mathbf{z}} \frac{1}{2} \|\mathbf{W}\mathbf{z} - \mathbf{x}\|_2^2 + \lambda \|\mathbf{z}\|_1$  with the proximal gradient descent method that projects the solution of each iteration into an  $l_1$ -ball by adopting the soft threshold function. However, because our **Definition 3** requires a simplex

mapping function  $P$ , we shrink the solution domain from an  $l_1$ -ball to a unit simplex  $\Delta_k^u$  to remove unexpected solutions for faster computation. This derives the following problem

$$\underset{\mathbf{z} \in \mathbb{R}_+^k}{\text{minimize}} \quad \frac{1}{2} \|\mathbf{W}\mathbf{z} - \mathbf{x}\|_2^2 + \lambda(\mathbf{z}^T \mathbf{1}_k - 1), \quad (9)$$

where  $\lambda \in \mathbb{R}_+$ . This problem can be solved by the projected gradient descent with the orthogonal projection operator as

$$\mathbf{z} \leftarrow S_\lambda(\mathbf{z} - \mathbf{W}^T(\mathbf{W}\mathbf{z} - \mathbf{x})). \quad (10)$$

where  $S_\theta(\mathbf{a}) : \mathbb{R}^k \rightarrow \mathbb{R}_+^k$  for a vector  $\mathbf{a} \in \mathbb{R}^k$  is the orthogonal projection operator onto the unit simplex, which is defined as  $S_\theta(\mathbf{a}) := \max(\mathbf{0}, \mathbf{a} - \theta)$ . We present the derivation of this operator in the supplementary file. Figure 2 (b) shows the overview of our framework. In our framework, Eq. (10) is represented as a near-one-hot encoding layer. Our near-one-hot encoder for  $P_o$  consists of  $L$  sequentially connected near-one-hot encoding layers to generate  $\mathbf{z}$ , where  $L$  denotes the number of layers. We also include a multilayer perceptron network (MLP) to evaluate  $\lambda$  for each input as deep K-SVD does.

## 5 Numerical Evaluation

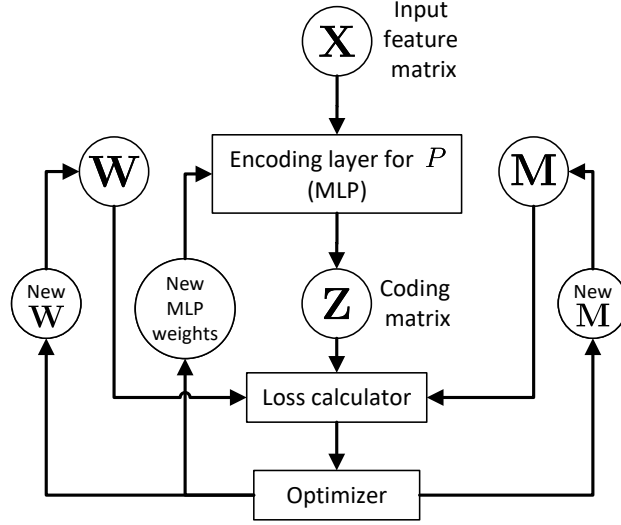
We conduct numerical experiments through three aspects: (i) distance approximation evaluation, (ii) computational time evaluation, and (iii) ablation studies of main parameter  $k$ . This section presents the our experimental reports.

### 5.1 Experimental setups

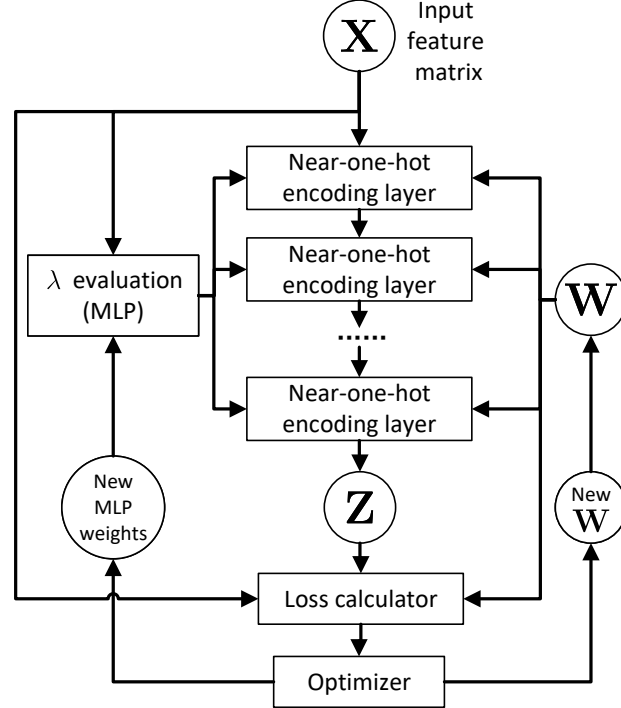
**Datasets.** We report our experiments on seven real-world graph datasets: MUTAG [25], PTC-MR [26], ENZYMES [27], BZR, COX2 [28], NCI1[29] and ZINC [30] from the TUdataset [31]. ZINC is a large-scale dataset containing 249456 graphs. For detailed statistical information about each graph dataset, please refer to the supplementary file. Furthermore, we also report experiments on a computer vision dataset: MNIST [32]. The MNIST database contains two splits: train and test subsets, where the train subset has 60000 images of handwritten digits from 0 to 9, while the test subset has 10000 images. Each of these images is resized into a  $28 \times 28$  matrix.

**Preprocessing on graph datasets.** Because the node features of the datasets are one-hot vectors of discrete labels, which are too simple for evaluating approximation performance. Therefore, to generate more complicated features, we conduct a feature updating preprocessing before training. More concretely, We conduct a classic message-passing-based updating equation as follows to update node features:  $\mathbf{x}'_i = (1 + \epsilon) \cdot \mathbf{x}_i + \sum_{j \in \mathcal{N}(i)} \mathbf{x}_j$ , where  $\mathcal{N}(i)$  denotes the set of indices of adjacent node of  $i$ -th node,  $\mathbf{x}_i \in \mathbb{R}^d$  denotes the feature of  $i$ -th node and  $\mathbf{x}'_i \in \mathbb{R}^d$  denotes its updated feature. This is exactly the updating equation of the famous graph isomorphism network [33] without the MLP layer. Specifically, we set the  $\epsilon = 0$ . For every data, we compute four times of updating equations iteratively. The final feature for each node will be the concatenation of its original feature and outputs of each iteration as  $[\mathbf{x}_i, \mathbf{x}'_i, \mathbf{x}''_i, \mathbf{x}'''_i, \mathbf{x}''''_i] \in \mathbb{R}^{5d}$ .

**Preprocessing on MNIST dataset.** We conduct a preprocessing operation on MNIST dataset to convert the image data into size-variable distributions. In the preprocessing, we only sample the pixels with non-zero values from the image. More concretely, assume  $i, j \in [28]$ , let  $p(i, j) \in [256]$  be the pixel value of  $i$ -th row and  $j$ -th column. Each image data is convert to a discrete distribution with 3-dimensional sampling points as  $\{[\frac{i}{28}, \frac{j}{28}, \frac{p(i,j)}{256}] \in \mathbb{R}^3 : i, j \in [28], p(i, j) > 0\}$ . Because we only sample pixels with values larger than 0, sizes of these distributions are variable.



(a) Deep metric learning ASOT



(b) Deep dictionary learning ASOT

Figure 2: The overall framework of our proposed deep anchor space learning methods, where  $\mathbf{X} \in \mathbb{R}^{n \times d}$  denotes the input feature matrix of sampling points,  $\mathbf{Z} = P(\mathbf{X})$  denotes the coding matrix mapped by  $P$ ,  $\mathbf{W} \in \mathbb{R}^{k \times d}$  denotes the anchor point matrix and  $\mathbf{M} \in \mathbb{R}^{h \times k}$  denotes the parameter matrix for metric learning. The mapping function  $P$  of ASOT-ML from (a) is parameterized with an MLP with output normalization, while  $P$  of ASOT-DL from (b) consists of several near-one-hot encoding layers, each of them computes one iteration of Eq. (10) with an adapted  $\lambda$  evaluated by an MLP.

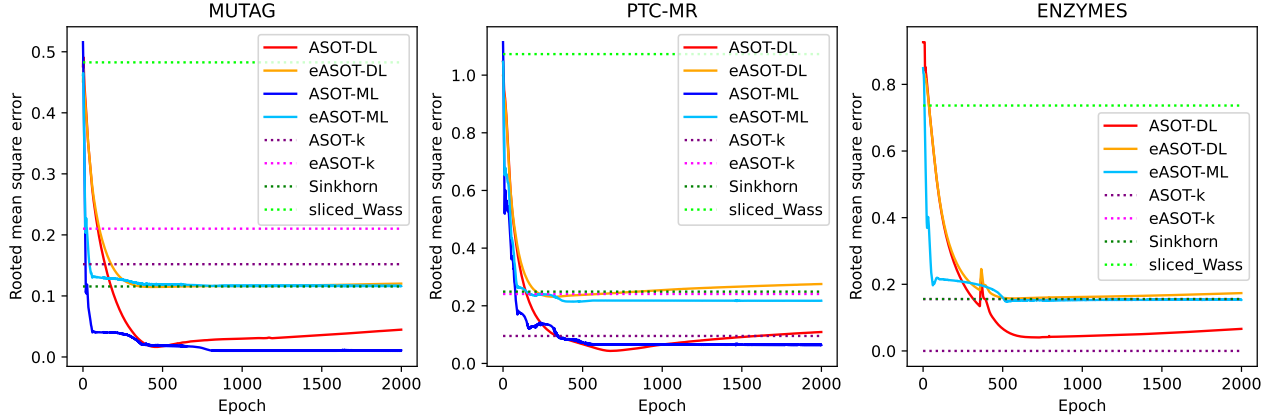


Figure 3: Average approximation error curves of graph datasets.

Table 1: Average approximation errors of graph datasets (RMSE).

Methods	MUTAG	PTC-MR	ENZYMES	BZR	COX2	NCI1	ZINC	MNIST
SW (CPU)	0.4826	1.0729	0.3253	0.3305	0.3253	0.6061	0.5761	0.1084
eOT (CPU)	0.1155	0.2489	0.1556	0.1366	0.0827	0.0791	0.0754	0.0981
BDS-eOT (GPU)	0.1035	0.0675	0.1487	0.1359	0.0807	0.0771	0.0744	-
ASOT-ML (CPU)	0.0264	0.0736	0.0554	0.0144	0.0058	0.0168	0.0306	0.0860
ASOT-DL (CPU)	0.0292	0.1037	0.0724	0.0296	0.0293	0.0293	0.0747	0.0972
ASOT- $k$ (CPU)	0.0862	0.1497	0.0287	0.0285	0.0256	0.0808	0.0410	0.0112
eASOT-ML (GPU)	0.1213	0.2211	0.1793	0.1367	0.0803	0.0810	0.0871	0.0766
eASOT-DL (GPU)	0.1160	0.2445	0.1685	0.1333	0.0905	0.0965	0.0773	0.0990
eASOT- $k$ (GPU)	0.1591	0.2318	0.1752	0.1476	0.0940	0.1229	0.0952	0.0766

Table 2: Average computational time cost of graph datasets (sec). For ASOT methods, the value at the left of “+” denotes the average training time, the one on the right denotes the distance computation time.

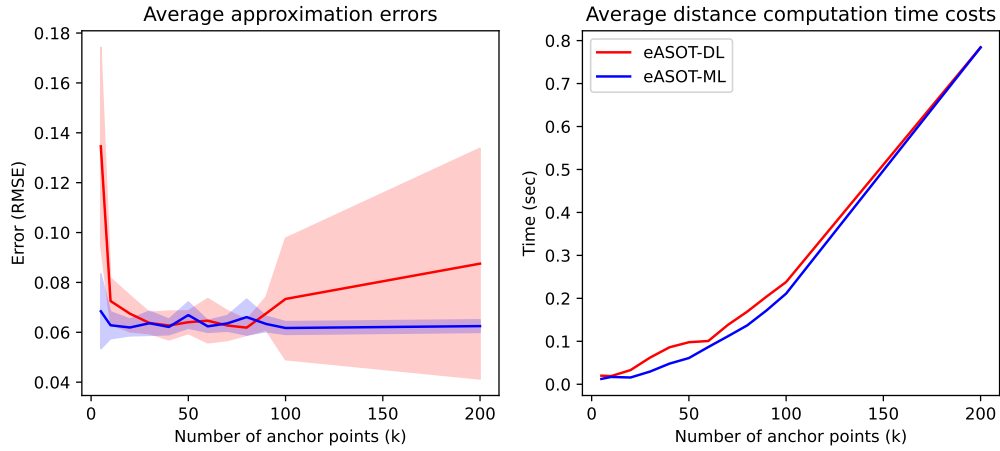
Methods	MUTAG	PTC-MR	ENZYMES	BZR	COX2	NCI1	ZINC	MNIST
OT-EMD (CPU)	2.00	6.72	27.54	16.36	28.12	1717	2566	190.4
SW (CPU)	2.59	13.45	23.53	91.45	62.05	4512	5190	25.92
eOT (CPU)	40.73	123.1	392.2	173.1	242.1	18574	29090	572.5
BDS-eOT (GPU)	6.78	26.34	85.36	42.48	56.42	3970	5703	-
ASOT-ML (CPU)	1.98+2.28	2.59+18.67	1.52+191.4	8.01+21.87	12.83+27.86	3.54+6871	1.95+2079	0.35+456.8
ASOT-DL (CPU)	5.97+1.84	6.07+7.20	5.86+24.46	5.12+10.77	4.78+21.34	7.09+1259	0.41+1458	0.96+366.1
ASOT- $k$ (CPU)	0.08+2.66	0.10+8.28	0.18+32.28	0.20+12.98	0.21+12.65	0.87+1103	33.22+1435	0.008+88.65
eASOT-ML (GPU)	1.98+0.03	2.59+0.31	1.52+2.46	8.01+0.20	12.83+0.28	3.54+93.63	1.95+16.43	<b>0.35+9.36</b>
eASOT-DL (GPU)	5.97+0.08	6.07+0.38	5.86+2.23	5.12+0.50	4.78+0.32	<b>7.09+18.30</b>	<b>0.41+16.60</b>	0.96+9.31
eASOT- $k$ (GPU)	<b>0.08+0.64</b>	<b>0.10+0.88</b>	<b>0.18+3.15</b>	<b>0.20+0.91</b>	<b>0.21+0.89</b>	0.87+86.44	33.22+16.96	0.008+9.91

**Baselines and other setups.** We set the Earth Movers Distance (OT-EMD) solved by [34] as the baseline distance, which computes an exact solution of the OT problem in Eq. (1) in the form of linear programming problem. For our proposed methods, except for ASOT-ML and ASOT-DL, we also implement a variant whose anchor space is learned by  $k$ -means according to **Proposition 2**. eASOT-ML, eASOT-DL, and eASOT-k denote the entropic ASOT solved by Sinkhorn’s solver with GPU-parallelization for ASOT-ML, ASOT-DL and the  $k$ -means variant, respectively. ASOT-ML, ASOT-DL, and ASOT-k denote the ones with EMD solver. For other compared approximate methods, we choose the followings: the entropic OT with the Sinkhorn’s algorithm [2] on CPU (eOT), the entropic OT with the Sinkhorn’s algorithm and the block diagonal stacking on GPU (BDS-eOT), and the sliced Wasserstein distance (SW) [9]. For the parameter settings of other methods, we use a Sinkhorn’s solver with  $\varepsilon = 0.1$  and 50 iterations, a sliced Wasserstein distance solver with  $d$  projections. For our methods, we set the number of anchor points  $k$  equal to the maximum number of nodes that a graph contains of the dataset. For the weights of losses of ASOT-DL, we set  $\alpha = 1, \beta = 1, \gamma = 1$ . For ASOT-ML, we set  $C = 100$ . More detailed parameter settings are provided in the supplementary file. We conduct 500 epochs of training with a batch size of 500 (graphs), except for ZINC, we only compute 50 epochs. For the subset division of graph datasets, we run a 10-fold cross-validation where train vs. test is 9 : 1, except for ZINC, where we use the default splits. We compute the pairwise distance of the whole dataset (train + test) for evaluation, except for ZINC, where we only compute the test subset. For the subset division of the MNIST dataset, we randomly choose 50 images for each category of digits from the test subset, with which we construct a subset of 500 images. We conduct 10 times of distance approximation experiments on these subsets, which are randomly generated with different random seeds for each run. The machine for experiments is equipped with an Intel CPU i7-12700KF, 32 GB RAM, and a GPU of NVIDIA GeForce RTX 3090Ti.

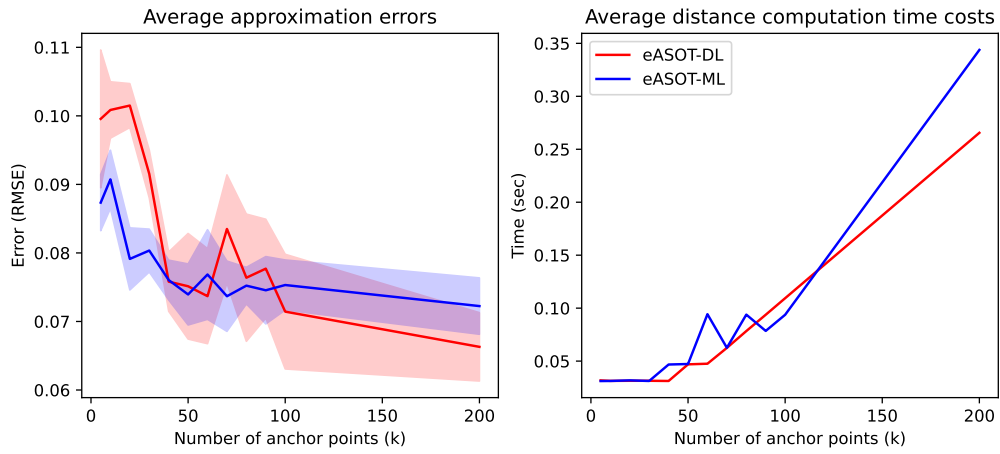
## 5.2 Wasserstein distance approximation

**Distance approximation evaluation.** In this experiments, we simulate a general task of pairwise Wasserstein distance matrix computation, where the distance between two graphs (images) is defined as the 1-Wasserstein distance with a Euclidean ground metric between their node feature sets (pixel feature sets). For the evaluation criterion, we adopt the rooted mean square error (RMSE) between approximated distance matrices and the ground truth computed by EMD. Figures 3 shows the curves of approximation errors of three graph datasets, where we can see both the eASOT-DL and eASOT-ML show great performance, which is very close to eOT and BDS-eOT. Table 1 shows the average approximation errors. We omit the standard deviations here but provide them in the supplementary file because all of them are less than 0.05.

**Computational time cost evaluation.** We also record and evaluate the distance computation time cost in the distance approximation experiments. Table 2 shows the time records of the computation of distance matrices in seconds, where the fastest one is with bold typeface. Our proposed eASOT-ML, eASOT-DL, and eASOT-k with GPU parallelization show amazing advantages on time cost compared to other conventional methods. We can observe that, on some datasets, the time cost of eASOT-ML or ASOT-ML is larger than the one of eASOT-DL or ASOT-DL, which fits our prediction that ASOT-ML may compute unsafe solutions that increase the number of required solving iterations. We provide the model training time costs in the supplementary file, which are also low costs with GPU parallelization.



(a) MUTAG dataset (graph)



(b) MNIST dataset (computer vision)

Figure 4: Average approximation error and computational time cost curves of an ablation study of the parameter  $k$ , where we report the results of a series of  $k$  of [5, 10, 20, 30, 40, 50, 60, 70, 80, 90, 100, 200].



### 5.3 Ablation studies

As described in previous sections, the parameter  $k$  is considered the most important parameter of our proposed ASOT, which denotes the number of learnable anchor points. In order to study how the approximation error deteriorates and computational time decreases with different  $k$ , we report two ablation study experiments on two different datasets: the graph dataset MUTAG and the computer vision dataset MNIST. We prepare a candidate set of  $k$  as [5, 10, 20, 30, 40, 50, 60, 70, 80, 90, 100, 200]. For each dataset, we conduct 5 runs of a single experiment and then report the means and standard deviations of the approximation error. We keep the experimental setups as the same as described in Section 5.1, except for the number of the Sinkhorn iterations, which we set as 200 for MUTAG and 500 for MNIST. Figure 4 shows the experimental results of approximation error and computational time with different  $k$ . From the curves one can observe a relatively stable descend of the approximation error curves of eASOT-ML on the both datasets, while the one of eASOT-DL shows signs of rebound on MUTAG dataset when  $k$  is larger than 90. We believe that this is because eASOT-DL optimize a loss which is a upper bound of the one of eASOT-ML, which make it easier to reach the limits and thus easier to overfit.

## 6 Conclusion

This paper presents a translation of the OT problem into an ASOT problem to accelerate batch processing of multiple OT problems, with taking advantages of the potential common characteristics of distributions. In the proposed ASOT, we only transport masses over a learned and fixed anchor space. We then prove the upper bound of the Wasserstein distance approximation error of such ASOT problem. Based on this, we propose a metric learning (ASOT-ML), a  $k$ -means-based (ASOT- $k$ ) and a deep dictionary learning framework (ASOT-DL) for anchor space learning. Experimental results demonstrate that our methods significantly decrease computational time while maintaining a reasonable level of approximation performance. For future work, we aim to design closed-form expressions for the mapping function and metric function of ASOT, eliminating the requirement for anchor space learning.

## A Proofs and derivation

This section provides the proofs of **Lemma 1**, **Proposition 1**, **Proposition 2**, and a derivation of Eq. (9) of the main paper. For mathematical notations, we follow what we have described in Section 2 of the main paper.

### A.1 Proof of Lemma 1

*Proof.* Let  $\mathbf{C}_s \in \mathbb{R}^{k \times k}$  denote a  $k \times k$  cost matrix. Let  $\mathbf{Z}_x \in \mathbb{R}^{n \times k}$ ,  $\mathbf{Z}_y \in \mathbb{R}^{m \times k}$ , where each row of  $\mathbf{Z}_x$  and  $\mathbf{Z}_y$  is a simplex vector. Assume an OT problem over discrete distributions with probability vectors  $\mathbf{a} \in \Delta_n^p$ ,  $\mathbf{b} \in \Delta_m^p$  as follows.

$$W_1 = \underset{\mathbf{T} \in \mathcal{U}(\mathbf{a}, \mathbf{b})}{\text{minimize}} \langle \mathbf{T}, \widehat{\mathbf{C}} \rangle,$$

where  $\widehat{\mathbf{C}} \in \mathbb{R}^{n \times m}$  can be decomposed into  $\widehat{\mathbf{C}} = \mathbf{Z}_x \mathbf{C}_s \mathbf{Z}_y^T$ . Then we have

$$\begin{aligned} W_1 &= \underset{\mathbf{T} \in \mathcal{U}(\mathbf{a}, \mathbf{b})}{\text{minimize}} \sum_{i \in [n], j \in [m]} \mathbf{T}(i, j) \cdot \widehat{\mathbf{C}}(i, j) \\ &= \underset{\mathbf{T} \in \mathcal{U}(\mathbf{a}, \mathbf{b})}{\text{minimize}} \sum_{i \in [n], j \in [m]} \mathbf{T}(i, j) \cdot \left( \sum_{u, v \in [k]} \mathbf{Z}_x(i, u) \mathbf{Z}_y(j, v) \mathbf{C}_s(u, v) \right) \\ &= \underset{\mathbf{T} \in \mathcal{U}(\mathbf{a}, \mathbf{b})}{\text{minimize}} \sum_{i \in [n], j \in [m]} \sum_{u, v \in [k]} \mathbf{Z}_x(i, u) \cdot \mathbf{Z}_y(j, v) \cdot \mathbf{T}(i, j) \cdot \mathbf{C}_s(u, v) \\ &= \underset{\mathbf{T} \in \mathcal{U}(\mathbf{a}, \mathbf{b})}{\text{minimize}} \sum_{u, v \in [k]} \left( \sum_{i \in [n], j \in [m]} \mathbf{Z}_x(i, u) \cdot \mathbf{Z}_y(j, v) \cdot \mathbf{T}(i, j) \right) \cdot \mathbf{C}_s(u, v). \end{aligned}$$

Let  $\mathbf{T}_s = \mathbf{Z}_x^T \mathbf{T} \mathbf{Z}_y \in \mathbb{R}^{k \times k}$ , the above equations can be converted as follows.

$$W_1^u = \underset{\mathbf{T} \in \mathcal{U}(\mathbf{a}, \mathbf{b})}{\text{minimize}} \langle \mathbf{T}_s, \mathbf{C}_s \rangle. \quad (11)$$

To reparameterize this problem with  $\mathbf{T}_s$ , we have to find the domain of  $\mathbf{T}_s$ . Right multiplying  $\mathbf{T}_s$  with  $\mathbf{1}_k$  obtains

$$\mathbf{T}_s \mathbf{1}_k = \mathbf{Z}_x^T \mathbf{T} \mathbf{Z}_y \mathbf{1}_k. \quad (12)$$

Because each row of  $\mathbf{Z}_y$  is a simplex vector, we have  $\mathbf{Z}_y \mathbf{1}_k = \mathbf{1}_m$ . Substituting it into Eq. (12) obtains

$$\mathbf{T}_s \mathbf{1}_k = \mathbf{Z}_x^T \mathbf{T} \mathbf{1}_m = \frac{1}{n} \mathbf{Z}_x^T \mathbf{a}.$$

In the same way, we can obtain  $\mathbf{T}_s^T \mathbf{1}_k = \frac{1}{m} \mathbf{Z}_y^T \mathbf{b}$ . Furthermore, because for all  $i \in [n], j \in [m]$ , we have  $\mathbf{T}(i, j) \geq 0$ , then  $\forall u, v \in [k]$ ,  $\mathbf{T}_s(u, v) \geq 0$  holds. In summary,  $\mathbf{T}_s \in \mathcal{U}(\mathbf{a}', \mathbf{b}')$ , where

$$\mathbf{a}' = \frac{1}{n} \mathbf{Z}_x^T \mathbf{a} = \frac{1}{n} \sum_{i=1}^n \mathbf{Z}_x(i, \cdot) \mathbf{a}(i), \quad \mathbf{b}' = \frac{1}{m} \mathbf{Z}_y^T \mathbf{b} = \frac{1}{m} \sum_{j=1}^m \mathbf{Z}_y(j, \cdot) \mathbf{b}(j).$$

Finally, Eq. (11) is reparameterized as

$$W_1 = \underset{\mathbf{T}_s \in \mathcal{U}(\mathbf{a}', \mathbf{b}')}{\text{minimize}} \langle \mathbf{T}_s, \mathbf{C}_s \rangle. \quad (13)$$

Give  $\mathcal{X}, \mathcal{Y}, \mathcal{W}$ , mapping function  $P$ , and metric function  $d_{AS}$  as defined in **Definition 3**, which satisfy  $\forall u, v \in [k], \mathbf{C}_s(u, v) = d_{AS}(\mathbf{w}_u, \mathbf{w}_v)$  and  $\forall i \in [n], \mathbf{Z}_x(i, \cdot) = P(\mathbf{x}_i)$  and  $\forall j \in [m], \mathbf{Z}_x(j, \cdot) = P(\mathbf{x}_j)$ . Then Eq. (13) is an ASOT problem of  $W_{AS}(\mathcal{D}_x, \mathcal{D}_y, \mathcal{W}, P, d_{AS})$ , which completes the proof.  $\square$

## A.2 Proof of Proposition 1

*Proof.* According to **Lemma 1**, the ASOT problem of  $W_{AS}(\mathcal{D}_x, \mathcal{D}_y, \mathcal{W}, P, d_{AS})$  is equivalent to the OT problem defined in Eq. (7). Let  $\hat{\mathbf{T}}^*$  be the optimal parameter of the equivalent OT problem in Eq. (7), let  $\mathbf{T}^*$  be the optimal parameter of the original OT problem of  $W_1(\mathcal{D}_x, \mathcal{D}_y, d_S)$ . we have

$$\begin{aligned} |W_{AS} - W_1| &:= |W_{AS}(\mathcal{D}_x, \mathcal{D}_y, \mathcal{W}, P, d_{AS}) - W_1(\mathcal{D}_x, \mathcal{D}_y, d_S)| \\ &= \left| \langle \hat{\mathbf{T}}^*, \hat{\mathbf{C}} \rangle - \langle \mathbf{T}^*, \mathbf{C} \rangle \right| \\ &= \left| \sum_{i \in [n], j \in [m]} \hat{\mathbf{T}}^*(i, j) \hat{\mathbf{C}}(i, j) - \sum_{i \in [n], j \in [m]} \mathbf{T}^*(i, j) \mathbf{C}(i, j) \right|. \end{aligned}$$

In the case of  $W_{AS}(\mathcal{D}_x, \mathcal{D}_y, \mathcal{W}, P, d_{AS}) > W_1(\mathcal{D}_x, \mathcal{D}_y, d_S)$ , we have

$$\begin{aligned} |W_{AS} - W_1| &= \sum_{i \in [n], j \in [m]} \hat{\mathbf{T}}^*(i, j) \hat{\mathbf{C}}(i, j) - \sum_{i \in [n], j \in [m]} \mathbf{T}^*(i, j) \mathbf{C}(i, j) \\ &\leq \sum_{i \in [n], j \in [m]} \mathbf{T}^*(i, j) \hat{\mathbf{C}}(i, j) - \sum_{i \in [n], j \in [m]} \mathbf{T}^*(i, j) \mathbf{C}(i, j) \\ &\leq \sum_{i \in [n], j \in [m]} \mathbf{T}^*(i, j) \left( \hat{\mathbf{C}}(i, j) - \mathbf{C}(i, j) \right), \end{aligned}$$

which is because OT problem is convex, its optimal solution is the global minima. Moreover, because  $\mathbf{T}^* \in \mathcal{U}(\mathbf{a}, \mathbf{b})$  and  $\mathbf{a}, \mathbf{b}$  are both in the probability simplexes, we have  $\sum_{i \in [n], j \in [m]} \mathbf{T}^*(i, j) = \|\mathbf{a}\|_1 = \|\mathbf{b}\|_1 = 1$ . Then we have

$$\begin{aligned} |W_{AS} - W_1| &\leq \sum_{i \in [n], j \in [m]} \mathbf{T}^*(i, j) \left( \hat{\mathbf{C}}(i, j) - \mathbf{C}(i, j) \right) \\ &\leq \sum_{i \in [n], j \in [m]} \mathbf{T}^*(i, j) \left| \hat{\mathbf{C}}(i, j) - \mathbf{C}(i, j) \right| \\ &< \|\hat{\mathbf{C}} - \mathbf{C}\|_\infty \\ &< \|\hat{\mathbf{C}} - \mathbf{C}\|_1. \end{aligned}$$

In the case of  $W_{AS}(\mathcal{D}_x, \mathcal{D}_y, \mathcal{W}, P, d_{AS}) \leq W_1(\mathcal{D}_x, \mathcal{D}_y, d_S)$ , we have

$$\begin{aligned} |W_{AS} - W_1| &= \sum_{i \in [n], j \in [m]} \mathbf{T}^*(i, j) \mathbf{C}(i, j) - \sum_{i \in [n], j \in [m]} \hat{\mathbf{T}}^*(i, j) \hat{\mathbf{C}}(i, j) \\ &\leq \sum_{i \in [n], j \in [m]} \hat{\mathbf{T}}^*(i, j) \left( \mathbf{C}(i, j) - \hat{\mathbf{C}}(i, j) \right) \\ &\leq \sum_{i \in [n], j \in [m]} \hat{\mathbf{T}}^*(i, j) \left| \mathbf{C}(i, j) - \hat{\mathbf{C}}(i, j) \right| \\ &< \|\mathbf{C} - \hat{\mathbf{C}}\|_\infty \\ &< \|\mathbf{C} - \hat{\mathbf{C}}\|_1. \end{aligned}$$

Combining the results of both cases above completes the proof.  $\square$

### A.3 Proof of Proposition 2

Before proving **Proposition 2**, we first prove the following theorem.

**Theorem 1.** *The function of  $l_2$  norm on an  $\mathbb{R}^d$  vector space, denoted as  $f(\mathbf{x}) := \|\mathbf{x}\|_2$ , is 1-Lipschitz continuous w.r.t. the Euclidean metric.*

*Proof.* According to the reverse triangle inequality [22] we have

$$\begin{aligned} |f(\mathbf{x}) - f(\mathbf{y})| &= \left| \|\mathbf{x}\|_2 - \|\mathbf{y}\|_2 \right| \\ &\leq \|\mathbf{x} - \mathbf{y}\|. \end{aligned}$$

Therefore,  $f(\mathbf{x})$  is 1-Lipschitz continuous, which completes the proof.  $\square$

*Proof.* According to **Proposition 1**, we have  $|W_{\text{AS}}(\mathcal{D}_x, \mathcal{D}_y, \mathcal{W}, P_o, d_E) - W_1(\mathcal{D}_x, \mathcal{D}_y, d_E)| < \|\widehat{\mathbf{C}} - \mathbf{C}\|$ . Expanding this inequality obtains

$$\begin{aligned} |W_{\text{AS}} - W_1| &:= |W_{\text{AS}}(\mathcal{D}_x, \mathcal{D}_y, \mathcal{W}, P_o, d_E) - W_1(\mathcal{D}_x, \mathcal{D}_y, d_E)| \\ &< \|\widehat{\mathbf{C}} - \mathbf{C}\| \\ &< \sum_{i \in [n], j \in [m]} \left| \widehat{\mathbf{C}}(i, j) - \mathbf{C}(i, j) \right|_1. \end{aligned}$$

Because  $\widehat{\mathbf{C}}$  can be decomposed into  $\widehat{\mathbf{C}} = \mathbf{Z}_x \mathbf{C}_s \mathbf{Z}_y^T$  according to **Proposition 1**, we have

$$\begin{aligned} |W_{\text{AS}} - W_1| &< \sum_{i \in [n], j \in [m]} \left| \widehat{\mathbf{C}}(i, j) - \mathbf{C}(i, j) \right| \\ &= \sum_{i \in [n], j \in [m]} \left| \sum_{u, v \in [k]} \mathbf{Z}_x(i, u) \cdot \mathbf{Z}_y(j, v) \cdot \mathbf{C}_s(u, v) - \mathbf{C}(i, j) \right| \\ &= \sum_{i \in [n], j \in [m]} \left| \sum_{u, v \in [k]} P_o(\mathbf{x}_i)(u) \cdot P_o(\mathbf{y}_j)(v) \cdot \mathbf{C}_s(u, v) - \mathbf{C}(i, j) \right|. \end{aligned}$$

Because  $P_o$  is an one-hot mapping function, we can let the index of non-zero element of  $P_o(\mathbf{x}_i)$  be  $u_i$ , and let the one of  $P_o(\mathbf{x}_i)$  be  $v_i$ . Substituting this into the equation above obtains

$$|W_{\text{AS}} - W_1| < \sum_{i \in [n], j \in [m]} |\mathbf{C}_s(u_i, v_j) - \mathbf{C}(i, j)|.$$

From **Definition 3**, we have  $\mathbf{C}_s(u_i, v_j) = d_S(\mathbf{w}_{u_i}, \mathbf{w}_{v_j}) = \|\mathbf{w}_{u_i} - \mathbf{w}_{v_j}\|_2$  and  $\mathbf{C}(i, j) = d_S(\mathbf{x}_i, \mathbf{y}_j) = \|\mathbf{x}_i - \mathbf{y}_j\|_2$ . Let  $\epsilon_i^x := \mathbf{W}P_o(\mathbf{x}_i) - \mathbf{x}_i$ ,  $\epsilon_j^y := \mathbf{W}P_o(\mathbf{y}_j) - \mathbf{y}_j$ . Then,  $\epsilon_i^x = \mathbf{w}_{u_i} - \mathbf{x}_i$ ,  $\epsilon_j^y = \mathbf{w}_{v_j} - \mathbf{y}_j$ . Substituting these into the inequality above obtains

$$\begin{aligned} |W_{\text{AS}} - W_1| &< \sum_{i \in [n], j \in [m]} \left| \|\mathbf{w}_{u_i} - \mathbf{w}_{v_j}\|_2 - \|(\mathbf{w}_{u_i} - \epsilon_i^x) - (\mathbf{w}_{v_j} - \epsilon_j^y)\|_2 \right| \\ &= \sum_{i \in [n], j \in [m]} \left| \|\mathbf{w}_{u_i} - \mathbf{w}_{v_j}\|_2 - \|(\mathbf{w}_{u_i} - \mathbf{w}_{v_j}) + (\epsilon_j^y - \epsilon_i^x)\|_2 \right|. \end{aligned}$$

According to **Theorem 1**, we have

$$\begin{aligned} |W_{\text{AS}} - W_1| &< \sum_{i \in [n], j \in [m]} \|\boldsymbol{\epsilon}_j^y - \boldsymbol{\epsilon}_i^x\|_2 = \sum_{i \in [n], j \in [m]} \|\boldsymbol{\epsilon}_j^y + (-\boldsymbol{\epsilon}_i^x)\|_2 \\ &\leq \sum_{i \in [n], j \in [m]} \|\boldsymbol{\epsilon}_j^y\|_2 + \|\boldsymbol{\epsilon}_i^x\|_2 = m \sum_{i \in [n]} \|\boldsymbol{\epsilon}_i^x\|_2 + n \sum_{j \in [m]} \|\boldsymbol{\epsilon}_j^y\|_2, \end{aligned}$$

which completes the proof.  $\square$

#### A.4 Derivation of Eq. (10)

Recall the primal problem that is expressed as

$$\underset{\mathbf{z} \in \mathbb{R}_+^k, \langle \mathbf{z}, \mathbf{1}_k \rangle \leq 1}{\text{minimize}} \left\{ f(\mathbf{z}) := \frac{1}{2} \|\mathbf{W}\mathbf{z} - \mathbf{x}\|_2^2 \right\}, \quad (14)$$

where we want to optimize a  $\mathbf{z}$  on the unit simplex  $\Delta_k^u$  that minimizes the squared reconstruction error. We first ignore the non-negative constraint  $\mathbf{z} \in \mathbb{R}_+^k$ , and we compute the Lagrangian of  $f(\mathbf{z})$  in Eq. (14) as follows.

$$L(\mathbf{z}, \lambda) := \frac{1}{2} \|\mathbf{W}\mathbf{z} - \mathbf{x}\|_2^2 + \lambda(\langle \mathbf{z}, \mathbf{1}_k \rangle - 1).$$

Assuming that the value of  $\lambda > 0$  is already known, the minimization of the above Lagrangian with respect to  $\mathbf{z} \in \mathbb{R}_+^k$  can be expressed as follows.

$$\underset{\mathbf{z} \in \mathbb{R}_+^k}{\text{minimize}} \frac{1}{2} \|\mathbf{W}\mathbf{z} - \mathbf{x}\|_2^2 + \langle \mathbf{z}, \lambda \mathbf{1}_k \rangle. \quad (15)$$

Let  $g(\mathbf{z}) = \langle \mathbf{z}, \lambda \mathbf{1}_k \rangle$ , according to the proximal gradient descent method [35], the update equation of  $\mathbf{z}$  with a fixed step size as 1 is expressed as follows.

$$\begin{aligned} \mathbf{z}^{(t+1)} &= \text{prox}_g(\mathbf{z}^{(t)} - \nabla f(\mathbf{z}^{(t)})) \\ &= \text{prox}_g(\mathbf{z}^{(t)} - \mathbf{W}^T(\mathbf{W}\mathbf{z}^{(t)} - \mathbf{x})), \end{aligned} \quad (16)$$

where  $\text{prox}_g$  denotes the proximal operator, which is defined as

$$\begin{aligned} \text{prox}_g(\mathbf{a}) &= \arg \min_{\mathbf{a}} g(\mathbf{a}) + \frac{1}{2} \|\mathbf{z} - \mathbf{a}\|_2^2 \\ &= \arg \min_{\mathbf{a}} \frac{1}{2} \|\mathbf{z} - \mathbf{a}\|_2^2 + \langle \mathbf{a}, \lambda \mathbf{1}_k \rangle \\ &= \arg \min_{\mathbf{a}} \sum_{i=1}^k \left( \frac{1}{2} (\mathbf{z}(i) - \mathbf{a}(i))^2 + \lambda \mathbf{a}(i) \right). \end{aligned} \quad (17)$$

Eq. (17) can be written as  $k$  subproblems with respect to each element of  $\mathbf{a}$ , such as

$$\text{prox}_g(\mathbf{a})(i) = \arg \min_{\mathbf{a}(i)} \frac{1}{2} (\mathbf{z}(i) - \mathbf{a}(i))^2 + \lambda \mathbf{a}(i).$$

Because of the non-negative condition of  $\mathbf{z}$  and Eq. (16), we have  $\forall i \in [k], \mathbf{a}(i) > 0$ . Therefore, the solutions of the above subproblems are  $\mathbf{a}(i) = \max(0, \mathbf{z}(i) - \lambda)$ . Generalizing these solutions to the vector  $\mathbf{a}$  yields

$$\text{prox}_g(\mathbf{a}) = \max(\mathbf{0}, \mathbf{a} - \lambda \mathbf{1}_k), \quad (18)$$

Table 3: Statistical information of datasets

Dataset	Dim.	Graphs	Avg. $ \mathcal{V} $	Avg. $ \mathcal{E} $	Max. $ \mathcal{V} $
MUTAG	7	188	17.93	19.79	28
PTC-MR	18	344	14.29	14.69	64
ENZYMES	3	600	32.63	62.14	126
BZR	53	405	35.75	38.35	57
COX2	35	467	41.22	43.45	56
NCI1	37	4110	29.86	32.30	111
ZINC	28	249456	23.15	24.90	38

Table 4: ASOT parameter settings

Parameters	ASOT-ML	ASOT-DL	ASOT- $k$
Num. of anchor points $k =  \mathcal{W} $	Max. $ \mathcal{V} $	Max. $ \mathcal{V} $	Max. $ \mathcal{V} $
Hidden dim. of Mahalanobis distance $h$	$d$	-	-
MLP for $P$ of ASOT-ML	$(5d, 10d, k)$	-	-
MLP for $\lambda$ evaluation of ASOT-DL	-	$(5d, 2.5d, 1)$	-
Num. of near-one-hot layers	-	20	-
$C$	100	-	-
$\alpha$	-	1.0	-
$\beta$	-	1.0	-
$\gamma$	-	1.0	-
Sinkhorn $\varepsilon$	0.1	0.1	0.1
Sinkhorn iterations	50	50	50
Optimizer	Adam[36]	Adam[36]	Mini-batch $k$ -means [37]
Learning rate	0.01	0.01	-

which derives the equation of our orthogonal projection operator  $S_\theta(\mathbf{a})$  of the paper. Substituting Eq. (18) into Eq. (16) yields

$$\mathbf{z}^{(t+1)} = S_\lambda(\mathbf{z}^{(t)} - \mathbf{W}^T(\mathbf{W}\mathbf{z}^{(t)} - \mathbf{x})), \quad (19)$$

which completes the derivation.

## B Details of graph experiments

This section describes the detailed settings and results of our numerical experiments on graph datasets, which are not included in our main paper.

**Detailed statistical information of graph datasets.** Table 3 records the statistical information of graph datasets used in our numerical experiments, where ‘‘Dim.’’ denotes the number of feature dimensions, ‘‘Avg.  $|\mathcal{V}|$ ’’ and ‘‘Avg.  $|\mathcal{E}|$ ’’ denote the average number of nodes and edges for a single graph, and ‘‘Max.  $|\mathcal{V}|$ ’’ denotes the maximum number of nodes for a single graph. Furthermore, ZINC dataset has a default splits of train and test subsets, whose sizes are 220011 and 5000, respectively.

Table 5: Standard deviations of approximation errors of graph datasets (RMSE).

Methods	MUTAG	PTC-MR	ENZYMES	BZR	COX2	NCI1	ZINC
ASOT-ML	0.0244	0.0164	0.0555	0.0015	0.0006	0.0022	0.0063
ASOT-DL	0.0104	0.0350	0.0370	0.0049	0.0081	0.0140	0.0137
ASOT- $k$	0.0455	0.0491	0.0863	0.0056	0.0256	0.0288	0.0053
eASOT- $k$	0.0343	0.0131	0.0587	0.0018	0.0075	0.0215	0.0039
eASOT-ML	0.0087	0.0271	0.0316	0.0011	0.0017	0.0004	0.0052
eASOT-DL	0.0045	0.0161	0.0146	0.0074	0.0087	0.0178	0.0040

Table 6: Average training time cost of graph datasets (sec).

Methods	MUTAG	PTC-MR	ENZYMES	BZR	COX2	NCI1	ZINC
ASOT-ML	1.98	2.59	1.52	8.01	12.83	3.54	1.95
ASOT-DL	5.97	6.07	5.86	5.12	4.78	7.09	0.41
ASOT- $k$	0.08	0.10	0.18	0.20	0.21	0.87	33.22

**Detailed ASOT parameter settings.** Table 4 records the parameter settings of ASOT-ML, ASOT-DL, and ASOT- $k$  in our graph experiments, where  $d$  denotes the number of dimensions of node features before preprocessing,  $\text{Max. } \mathcal{V}$  denotes the same one in Table 3. For the parameters we do not record in the main paper, we set the hidden dimensions of  $\mathbf{M} \in \mathbb{R}^{h \times k}$  equal to  $d$  in ASOT-ML. Furthermore, we parameterize  $P$  with a two-layer MLP with entries of  $(5d, 10d, k)$  in ASOT-ML. We also use another two-layer MLP with entries of  $(5d, 2.5d, 1)$  to evaluate  $\lambda$  in ASOT-DL.

**Standard deviations of approximation errors** Table 5 reports the standard deviations of approximation errors in our graph experiments, w.r.t. the average errors in Table 1 of the main paper.

**Training time costs.** Table 6 reports the average training time costs of our ASOT methods on different graph datasets. Training time costs in ZINC is less than other datasets because we only conduct 50 epochs of training on ZINC, while we train 500 epochs on other datasets. From the table, we can see that ASOT-ML is faster than ASOT-DL on small datasets such as MUTAG, PTC-MR, and ENZYMES. This is because ASOT-DL includes 20 near-one-hot layers for  $P$  while ASOT-ML only has a two-layer MLP encoder, which will cost more training time.

## References

- [1] Cédric Villani. Optimal transport: Old and new. Springer, New York, 2008.
- [2] Gabriel Peyré and Marco Cuturi. Computational optimal transport. Foundations and Trends in Machine Learning, 11(5-6):355–607, 2019.
- [3] Martin Arjovsky, Soumith Chintala, and Léon Bottou. Wasserstein generative adversarial networks. In International Conference on Machine Learning (ICML), 2017.

- [4] Aude Genevay, Gabriel Peyré, and Marco Cuturi. Learning generative models with Sinkhorn divergences. In International Conference on Artificial Intelligence and Statistics (AISTATS), 2018.
- [5] Matteo Togninalli, Elisabetta Ghisu, Felipe Llinares-López, Bastian Rieck, and Karsten Borgwardt. Wasserstein Weisfeiler-Lehman graph kernels. In Annual Conference on Neural Information Processing Systems (NeurIPS), 2019.
- [6] Soheil Kolouri, Navid Naderializadeh, Gustavo K. Rohde, and Heiko Hoffmann. Wasserstein embedding for graph learning. In International Conference on Learning Representations (ICLR), 2021.
- [7] Bing Su and Gang Hua. Order-preserving Wasserstein distance for sequence matching. In Proceedings of the IEEE conference on computer vision and pattern recognition (CVPR), 2017.
- [8] Mitsuhiko Horie and Hiroyuki Kasai. Auto-weighted sequential Wasserstein distance and application to sequence matching. In European Signal Processing Conference (EUSIPCO), 2022.
- [9] Nicolas Bonneel, Julien Rabin, Gabriel Peyré, and Hanspeter Pfister. Sliced and radon Wasserstein barycenters of measures. Journal of Mathematical Imaging and Vision, 51(1):22–45, 2015.
- [10] Soheil Kolouri, Kimia Nadjahi, Umut Simsekli, Roland Badeau, and Gustavo Rohde. Generalized sliced Wasserstein distances. In Annual Conference on Neural Information Processing Systems (NeurIPS), 2019.
- [11] Zhongxi Fang, Sun Xun Huang, Jianming, and Hiroyuki Kasai. Wasserstein graph distance based on L1-approximated tree edit distance between Weisfeiler-Lehman subtrees. In AAAI Conference on Artificial Intelligence (AAAI), 2023.
- [12] Jianming Huang, Zhongxi Fang, and Hiroyuki Kasai. LCS graph kernel based on Wasserstein distance in longest common subsequence metric space. Digital Signal Processing, 189:108281, 2021.
- [13] Jianbo Ye, Panruo Wu, James Z Wang, and Jia Li. Fast discrete distribution clustering using Wasserstein barycenter with sparse support. IEEE Transactions on Signal Processing, 65(9):2317–2332, 2017.
- [14] Takumi Fukunaga and Hiroyuki Kasai. Wasserstein  $k$ -means with sparse simplex projection. In International Conference on Pattern Recognition (ICPR), 2020.
- [15] Chi-Heng Lin, Mehdi Azabou, and Eva L Dyer. Making transport more robust and interpretable by moving data through a small number of anchor points. Proceedings of machine learning research, 139:6631, 2021.
- [16] François-Pierre Paty and Marco Cuturi. Subspace robust Wasserstein distances. In International Conference on Machine Learning (ICML), 2019.
- [17] Richard Sinkhorn and Paul Knopp. Concerning nonnegative matrices and doubly stochastic matrices. Pacific Journal of Mathematics, 21(2):343–348, 1967.
- [18] Marco Cuturi. Sinkhorn distances: Lightspeed computation of optimal transport. In Annual Conference on Neural Information Processing Systems (NeurIPS), 2013.



- [19] Jean-David Benamou, Guillaume Carlier, Marco Cuturi, Luca Nenna, and Gabriel Peyré. Iterative Bregman projections for regularized transportation problems. SIAM Journal on Scientific Computing, 37(2):1111–A1138, 2015.
- [20] Jason Altschuler, Jonathan Niles-Weed, and Philippe Rigollet. Near-linear time approximation algorithms for optimal transport via Sinkhorn iteration. In Annual Conference on Neural Information Processing Systems (NeurIPS), 2017.
- [21] Matthias Fey and Jan Eric Lenssen. Fast graph representation learning with pytorch geometric. arXiv preprint arXiv:1903.02428, 2019.
- [22] The Popular Educator, volume 4, page 196. John Cassel, 1855.
- [23] Meyer Scetbon, Michael Elad, and Peyman Milanfar. Deep K-SVD denoising. IEEE Transactions on Image Processing, 30:5944–5955, 2021.
- [24] Ingrid Daubechies, Michel Defrise, and Christine De Mol. An iterative thresholding algorithm for linear inverse problems with a sparsity constraint. Communications on Pure and Applied Mathematics: A Journal Issued by the Courant Institute of Mathematical Sciences, 57(11):1413–1457, 2004.
- [25] Asim Kumar Debnath, Rosa L Lopez de Compadre, Gargi Debnath, Alan J Shusterman, and Corwin Hansch. Structure-activity relationship of mutagenic aromatic and heteroaromatic nitro compounds. correlation with molecular orbital energies and hydrophobicity. Journal of medicinal chemistry, 34(2):786–797, 1991.
- [26] Christoph Helma, Ross D. King, Stefan Kramer, and Ashwin Srinivasan. The predictive toxicology challenge 2000–2001. Bioinformatics, 17(1):107–108, 2001.
- [27] Ida Schomburg, Antje Chang, Christian Ebeling, Marion Gremse, Christian Heldt, Gregor Huhn, and Dietmar Schomburg. BRENDA, the enzyme database: updates and major new developments. Nucleic acids research, 32(suppl\_1):D431–D433, 2004.
- [28] Jeffrey J Sutherland, Lee A O’Brien, and Donald F Weaver. Spline-fitting with a genetic algorithm: A method for developing classification structure-activity relationships. Journal of chemical information and computer sciences, 43(6):1906–1915, 2003.
- [29] Nikil Wale, Ian A Watson, and George Karypis. Comparison of descriptor spaces for chemical compound retrieval and classification. Knowledge and Information Systems, 14:347–375, 2008.
- [30] Xavier Bresson and Thomas Laurent. A two-step graph convolutional decoder for molecule generation. arXiv preprint arXiv:1906.03412, 2019.
- [31] Christopher Morris, Nils M. Kriege, Franka Bause, Kristian Kersting, Petra Mutzel, and Marion Neumann. TUDataset: A collection of benchmark datasets for learning with graphs. In International Conference on Machine Learning (ICML), 2020.
- [32] Yann LeCun. The MNIST database of handwritten digits. <http://yann.lecun.com/exdb/mnist/>, 1998.
- [33] Keyulu Xu, Weihua Hu, Jure Leskovec, and Stefanie Jegelka. How powerful are graph neural networks? In International Conference on Learning Representations (ICLR), 2019.

- [34] Nicolas Bonneel, Michiel Van De Panne, Sylvain Paris, and Wolfgang Heidrich. Displacement interpolation using lagrangian mass transport. In Proceedings of the Special Interest Group on Computer Graphics and Interactive Techniques (SIGGRAPH), 2011.
- [35] Neal Parikh, Stephen Boyd, et al. Proximal algorithms. Foundations and Trends in Optimization, 1(3):127–239, 2014.
- [36] Diederik P Kingma and Jimmy Ba. Adam: A method for stochastic optimization. In International Conference on Machine Learning (ICML), 2015.
- [37] David Sculley. Web-scale k-means clustering. In International Conference on World wide web (WWW), 2010.